[44] C. F. Semenkovich and J. W. Heinecke, "The mystery of diabetes and atherosclerosis: time for a new plot," *Diabetes*, vol. 46, no. 3, pp. 327–334, 1997.

[45] W. Lu, H. Takahashi, B. Furusato et al., "Allelotyping analysis at chromosome arm 8p of high-grade prostatic intraepithelial neoplasia and incidental, latent, and clinical prostate cancers," *Genes Chromosomes and Cancer*, vol. 45, no. 5, pp. 509–515, 2006.

[46] M. Gallucci, R. Merola, A. Farsetti et al., "Cytogenetic profiles as additional markers to pathological features in clinically localized prostate carcinoma," *Cancer Letters*, vol. 237, no. 1, pp. 76–82, 2006.

[47] G. S. Bova, B. S. Carter, M. J. G. Bussemakers et al., "Homozygous deletion and frequent allelic loss of chromosome 8p22 loci in human prostate cancer," *Cancer Research*, vol. 53, no. 17, pp. 3869–3873, 1993.

[48] J. Xu, S. L. Zheng, G. A. Hawkins et al., "Linkage and association studies of prostate cancer susceptibility: evidence for linkage at 8p22-23," *American Journal of Human Genetics*, vol. 69, no. 2, pp. 341–350, 2001.

[49] M. A. Knowles, J. S. Aveyard, C. F. Taylor, P. Harnden, and S. Bass, "Mutation analysis of the 8p candidate tumour suppressor genes DBC2 (RHOBTB2) and LZTS1 in bladder cancer," *Cancer Letters*, vol. 225, no. 1, pp. 121–130, 2005.

[50] T. J. Seng, J. S. W. Low, H. Li et al., "The major 8p22 tumor suppressor DLC1 is frequently silenced by methylation in both endemic and sporadic nasopharyngeal, esophageal, and cervical carcinomas, and inhibits tumor cell colony formation," *Oncogene*, vol. 26, no. 6, pp. 934–944, 2007.

[51] M. Di Benedetto, P. Pineau, S. Nouet et al., "Mutation analysis of the 8p22 candidate tumor suppressor gene ATIP/MTUS1 in hepatocellular carcinoma," *Molecular and Cellular Endocrinology*, vol. 252, no. 1-2, pp. 207–215, 2006.

[52] M. Di Benedetto, I. Bièche, F. Deshayes et al., "Structural organization and expression of human MTUS1, a candidate 8p22 tumor suppressor gene encoding a family of angiotensin II AT2 receptor-interacting proteins, ATIP," *Gene*, vol. 380, no. 2, pp. 127–136, 2006.

[53] S. Narita, N. Tsuchiya, L. Wang et al., "Association of lipoprotein lipase gene polymorphism with risk of prostate cancer in a Japanese population," *International Journal of Cancer*, vol. 112, no. 5, pp. 872–876, 2004.

[54] J. W. Kim, Y. Cheng, W. Liu et al., "Genetic and epigenetic inactivation of LPL gene in human prostate cancer," *International Journal of Cancer*, vol. 124, no. 3, pp. 734–738, 2009.

[55] J. Raju and R. P. Bird, "Energy restriction reduces the number of advanced aberrant crypt foci and attenuates the expression of colonic transforming growth factor β and cyclooxygenase isoforms in Zucker obese (fa/fa) rats," *Cancer Research*, vol. 63, no. 20, pp. 6595–6601, 2003.

[56] M. Ochiai, K. Ogawa, K. Wakabayashi et al., "Induction of intestinal adenocarcinomas by 2-amino-1-methyl-6-phenylimidazo-[4,5-b]pyridine in Nagase analbuminemic rats," *Japanese Journal of Cancer Research*, vol. 82, no. 4, pp. 363–366, 1991.

[57] N. Koohestani, T. T. Tran, W. Lee, T. M. S. Wolever, and W. R. Bruce, "Insulin resistance and promotion of aberrant crypt foci in the colons of rats on a high-fat diet," *Nutrition and Cancer*, vol. 29, no. 1, pp. 69–76, 1997.

[58] C. F. Quesada, H. Kimata, M. Mori, M. Nishimura, T. Tsuneyoshi, and S. Baba, "Piroxicam and acarbose as chemopreventive agents for spontaneous intestinal adenomas in APC gene 1309 knockout mice," *Japanese Journal of Cancer Research*, vol. 89, no. 4, pp. 392–396, 1998.

[59] N. Niho, M. Takahashi, T. Kitamura et al., "Concomitant suppression of hyperlipidemia and intestinal polyp formation in Apc-deficient mice by peroxisome proliferator-activated receptor ligands," *Cancer Research*, vol. 63, no. 18, pp. 6090–6095, 2003.

[60] N. Niho, M. Takahashi, Y. Shoji et al., "Dose-dependent suppression of hyperlipidemia and intestinal polyp formation in Min mice by pioglitazone, a PPARγ ligand," *Cancer Science*, vol. 94, no. 11, pp. 960–964, 2003.

[61] N. Teraoka, M. Mutoh, S. Takasu et al., "High susceptibility to azoxymethane-induced colorectal carcinogenesis in obese KK-A(y) mice," *International Journal of Cancer*, vol. 129, no. 3, pp. 528–535, 2011.

[62] Y. Yasui, R. Suzuki, S. Miyamoto et al., "A lipophilic statin, pitavastatin, suppresses inflammation-associated mouse colon carcinogenesis," *International Journal of Cancer*, vol. 121, no. 10, pp. 2331–2339, 2007.

[63] Y. Takeuchi, M. Takahashi, K. Sakano et al., "Suppression of N-nitrosobis(2-oxopropyl)amine-induced pancreatic carcinogenesis in hamsters by pioglitazone, a ligand of peroxisome proliferator-activated receptor γ," *Carcinogenesis*, vol. 28, no. 8, pp. 1692–1696, 2007.

[64] T. Tanaka, H. Kohno, R. Suzuki, Y. Yamada, S. Sugie, and H. Mori, "A novel inflammation-related mouse colon carcinogenesis model induced by azoxymethane and dextran sodium sulfate," *Cancer Science*, vol. 94, no. 11, pp. 965–973, 2003.

[65] N. Niho, M. Mutoh, M. Takahashi, K. Tsutsumi, T. Sugimura, and K. Wakabayashi, "Concurrent suppression of hyperlipidemia and intestinal polyp formation by NO-1886, increasing lipoprotein lipase activity in Min mice," *Proceedings of the National Academy of Sciences of the United States of America*, vol. 102, no. 8, pp. 2970–2974, 2005.

[66] N. Niho, M. Mutoh, M. Komiya, T. Ohta, T. Sugimura, and K. Wakabayashi, "Improvement of hyperlipidemia by indomethacin in Min mice," *International Journal of Cancer*, vol. 121, no. 8, pp. 1665–1669, 2007.

[67] K. Tsutsumi, Y. Inoue, A. Shima, K. Iwasaki, M. Kawamura, and T. Murase, "The novel compound NO-1886 increases lipoprotein lipase activity with resulting elevation of high density lipoprotein cholesterol, and long-term administration inhibits atherogenesis in the coronary arteries of rats with experimental atherosclerosis," *Journal of Clinical Investigation*, vol. 92, no. 1, pp. 411–417, 1993.

[68] M. Doi, Y. Kondo, and K. Tsutsumi, "Lipoprotein lipase activator NO-1886 (ibrolipim) accelerates the mRNA expression in fatty acid oxidation-related enzymes in rat liver," *Metabolism*, vol. 52, no. 12, pp. 1547–1550, 2003.

[69] T. Akasu, T. Yokoyama, K. Sugihara, S. Fujita, Y. Moriya, and T. Kakizoe, "Peroral sustained-release indomethacin treatment for rectal adenomas in familial adenomatous polyposis: a pilot study," *Hepato-Gastroenterology*, vol. 49, no. 47, pp. 1259–1261, 2002.

[70] C. H. Chiu, M. F. McEntee, and J. Whelan, "Discordant effect of aspirin and indomethacin on intestinal tumor burden in Apc(Min/+) mice," *Prostaglandins Leukotrienes and Essential Fatty Acids*, vol. 62, no. 5, pp. 269–275, 2000.

[71] N. Kusunoki, R. Yamazaki, and S. Kawai, "Induction of apoptosis in rheumatoid synovial fibroblasts by celecoxib, but not by other selective cyclooxygenase 2 inhibitors," *Arthritis and Rheumatism*, vol. 46, no. 12, pp. 3159–3167, 2002.

[72] R. S. Kota, C. V. Ramana, F. A. Tenorio, R. I. Enelow, and J. C. Rutledge, "Differential effects of lipoprotein lipase on tumor necrosis factor-α and interferon-γ-mediated gene expression in human endothelial cells," *Journal of Biological Chemistry*, vol. 280, no. 35, pp. 31076–31084, 2005.

[73] J. Yu, E. S. H. Chu, A. Y. Hui et al., "Lipoprotein lipase activator ameliorates the severity of dietary steatohepatitis," *Biochemical and Biophysical Research Communications*, vol. 356, no. 1, pp. 53–59, 2007.

[74] L. Lichtenstein, F. Mattijssen, N. J. De Wit et al., "Angptl4 protects against severe proinflammatory effects of saturated fat by inhibiting fatty acid uptake into mesenteric lymph node macrophages," *Cell Metabolism*, vol. 12, no. 6, pp. 580–592, 2010.

[75] S. Schwarz, B. Hufnagel, M. Dworak, S. Klumpp, and J. Krieglstein, "Protein phosphatase type 2Cα and 2Cβ are involved in fatty acid-induced apoptosis of neuronal and endothelial cells," *Apoptosis*, vol. 11, no. 7, pp. 1111–1119, 2006.

[76] I. J. Goldberg and M. Merkel, "Lipoprotein lipase: physiology, biochemistry, and molecular biology," *Frontiers in Bioscience*, vol. 6, pp. D388–405, 2001.

[77] R. Gruen, E. Hietanen, and M. R. C. Greenwood, "Increased adipose tissue lipoprotein lipase activity during the development of the genetically obese rat (fa/fa)," *Metabolism*, vol. 27, no. 12, supplement 2, pp. 1955–1966, 1978.

[78] R. S. Schwartz and J. D. Brunzell, "Increased adipose tissue lipoprotein lipase activity in moderately obese men after weight reduction," *The Lancet*, vol. 1, no. 8076, pp. 1230–1231, 1978.

[79] J. M. Ong and P. A. Kern, "Effect of feeding and obesity on lipoprotein lipase activity, immunoreactive protein, and messenger RNA levels in human adipose tissue," *Journal of Clinical Investigation*, vol. 84, no. 1, pp. 305–311, 1989.

[80] R. L. Seip, T. J. Angelopoulos, and C. F. Semenkovich, "Exercise induces human lipoprotein lipase gene expression in skeletal muscle but not adipose tissue," *American Journal of Physiology*, vol. 268, no. 2, pp. E229–E236, 1995.

[81] M. Kusunoki, T. Hara, K. Tsutsumi et al., "The lipoprotein lipase activator, NO-1886, suppresses fat accumulation and insulin resistance in rats fed a high-fat diet," *Diabetologia*, vol. 43, no. 7, pp. 875–880, 2000.

Cancer Science
The official journal of the Japanese Cancer Association JCA

Semaphorin 4D, a lymphocyte semaphorin, enhances tumor cell motility through binding its receptor, plexinB1, in pancreatic cancer

Shingo Kato,[1] Kensuke Kubota,[1] Takeshi Shimamura,[1] Yoshiyasu Shinohara,[1] Noritoshi Kobayashi,[1] Seitaro Watanabe,[1] Masato Yoneda,[1] Masahiko Inamori,[1] Fumio Nakamura,[2] Hitoshi Ishiguro,[3,4] Noboru Nakaigawa,[3] Yoji Nagashima,[5] Masataka Taguri,[6] Yoshinobu Kubota,[3] Yoshio Goshima,[2] Satoshi Morita,[6] Itaru Endo,[7] Shin Maeda,[1] Atsushi Nakajima[1,9] and Hitoshi Nakagama[8]

Departments of [1]Gastroenterology, [2]Molecular Pharmacology and Neurobiology, [3]Urology, Yokohama City University Graduate School of Medicine, Yokohama; [4]Photocatalyst Group, Kanagawa Academy of Science and Technology, Kawasaki; [5]Molecular Pathology, [6]Biostatistics and Epidemiology, [7]Gastroenterological Surgery, Yokohama City University Graduate School of Medicine, Yokohama, Kanagawa; [8]Division of Biochemistry, National Cancer Center Research, Institute, Chuo-ku, Tokyo, Japan

(Received June 15, 2011/Revised July 20, 2011/Accepted July 25, 2011/Accepted manuscript online August 4, 2011/Article first published online September 14, 2011)

Pancreatic ductal adenocarcinoma (PDAC) is a highly malignant tumor, for which the development of new biomarkers and therapeutic targets has become critical. The main cause of poor prognosis in PDAC patients is the high invasive and metastatic potential of the cancer. In the present study, we report a new signaling pathway that was found to mediate the enhanced tumor cell motility in pancreatic cancer. Semaphorin 4D (Sema4D) is a ligand known to be expressed on different cell types, and has been reported to be involved in the regulation of immune functions, epithelial morphogenesis, and tumor growth and metastasis. In this study, we revealed for the first time that the cancer tissue cells expressing Sema4D in PDAC are tumor-infiltrating lymphocytes. The overexpression of Sema4D and of its receptor, plexinB1, was found to be significantly correlated with clinical factors, such as lymph node metastasis, distant metastasis, and poor prognosis in patients with PDAC. Through *in vitro* analysis, we demonstrated that Sema4D can potentiate the invasiveness of pancreatic cancer cells and we identified the downstream molecules. The binding of Sema4D to plexinB1 induced small GTPase Ras homolog gene family, member A activation and resulted in the phosphorylation of MAPK and Akt. In addition, in terms of potential therapeutic application, we clearly demonstrated that the enhanced-cell invasiveness induced by Sema4D could be inhibited by knockdown of plexinB1, suggesting that blockade of plexinB1 might diminish the invasive potential of pancreatic cancer cells. Our findings provide new insight into possible prognostic biomarkers and therapeutic targets in PDAC patients. (*Cancer Sci* 2011; 102: 2029–2037)

Pancreatic ductal adenocarcinoma (PDAC) is the fourth leading cause of cancer death in the USA and the fifth in Japan, with an estimated 34 100 and 22 000 patients dying of this disease each year in the two countries, respectively.[1,2] Because of the aggressive growth characteristic and potential for early metastatic dissemination of PDAC, the overall 5-year survival rate of patients with this cancer is <5%. The poor prognosis of PDAC patients can be mainly attributed to the low curative resection rates; only 15–20% of patients have resectable PDAC because of the high frequency of distant metastases or severe local invasion present at diagnosis.[3] Thus, the intense invasive and metastatic potential of the tumor cells pose the greatest threats in patients with PDAC. In order to improve the dismal survival rate, it is necessary to clarify the signaling pathways that regulate the invasive potential of the pancreatic cancer cells. In the present study, we report a new signaling pathway that was found to mediate the enhanced tumor cell motility in pancreatic cancer.

Semaphorins are a large family of either membrane-bound or secreted proteins that were originally described in the nervous system, where they are involved in the establishment of accurate neural networks.[4,5] Most members of the semaphorin family have also been shown to be expressed outside the nervous system, and to be involved in the regulation of immune functions,[6,7] epithelial morphogenesis,[8] and tumor growth and metastasis.[9,10]

Semaphorin 4D (Sema4D) is a member of the class 4 membrane-bound semaphorins, and was previously called CD100, a human lymphocyte surface antigen initially found to be expressed in human T-cell clones.[11,12] Semaphorin 4D is the first human semaphorin known to be expressed in normal T and B lymphocytes, and its expression has been shown to be enhanced by lymphocyte activation.[13,14] It is now known that although Sema4D is a transmembrane protein, a soluble form is released from the cell surface by different cell types.[6] The high-affinity receptor of Sema4D is plexinB1,[15] and two pathways by which Sema4D enhances cell motility through plexinB1 have been reported: the first is transactivation of the tyrosine kinase activity of Met,[8] a tyrosine kinase receptor that mediates a complex program known as invasive growth,[16] and the other is the activation of small GTPase Ras homolog gene family, member A (RhoA)[17] and the phosphorylation of MAPK and Akt.[18]

A recent study on breast cancer showed that Sema4D can enhance the motility of cancer cells through binding plexinB1, and that in an environment lacking Sema4D, the potential of breast cancer cells to form tumor masses and to metastasize was severely impaired.[19] However, the precise role of Sema4D in pancreatic cancer has not yet been clarified.

In the present study, we attempted to determine the clinicopathological significance of the expressions of Sema4D and plexinB1 by examining surgically-resected specimens of PDAC and conducting functional analyses of pancreatic cancer cell lines. We obtained evidence suggesting that the activation of the Sema4D/plexin B1 signaling pathway could enhance tumor cell motility in pancreatic cancer. Furthermore, we also propose that the molecules of this signaling pathway can serve as potential therapeutic targets and prognostic markers in PDAC patients.

[9]To whom correspondence should be addressed.
E-mail: nakajima-tky@umin.ac.jp

doi: 10.1111/j.1349-7006.2011.02053.x

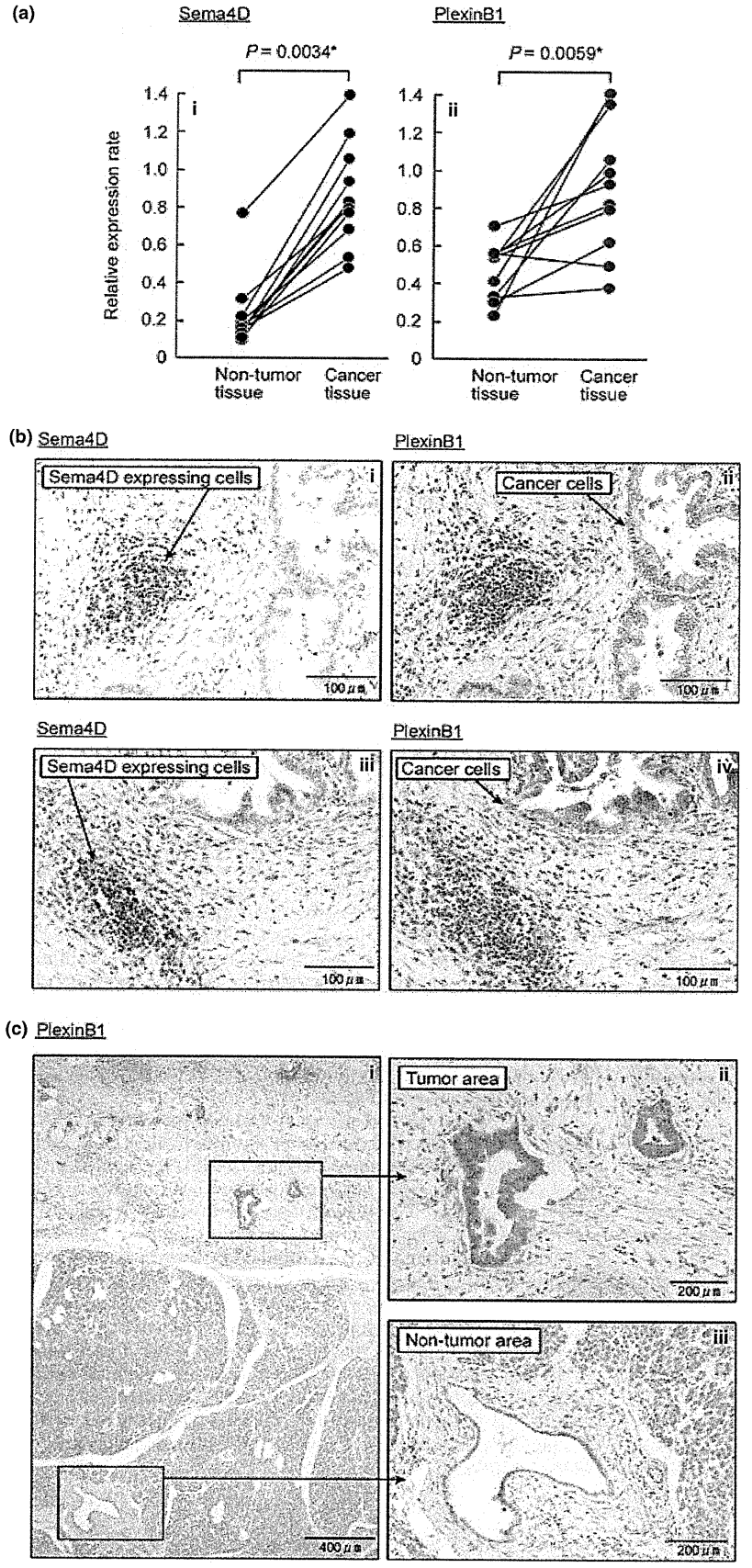

Fig. 1. Semaphorin 4D (Sema4D) and plexinB1 expressions in human pancreatic cancer tissues. (a) Semaphorin 4D and plexinB1 expressions were evaluated at the mRNA level in 11 surgically-resected specimens of human pancreatic cancer and paired normal pancreatic tissues. Both Sema4D and plexinB1 mRNA were significantly overexpressed in the pancreatic cancer tissues, as compared to those in the paired normal pancreatic tissues obtained from the same patients ($P = 0.0034$ & $P = 0.0059$, respectively). (b) Immunohistochemistry for Sema4D revealed that Sema4D was expressed in the cancer stroma, but not in the cancer epithelial cells. However, plexinB1 expression was observed in the cancer epithelial cells. (c) Strong plexinB1 expression was observed in the cancer epithelial cells, whereas its expression was only faint in the pancreatic ductal epithelial cells in the non-tumor area. In the immunohistochemistry scoring of plexinB1, we compared the staining intensity of cancer cells with that of the pancreatic ductal epithelial cells in the non-tumor area in the same patient.

doi: 10.1111/j.1349-7006.2011.02053.x

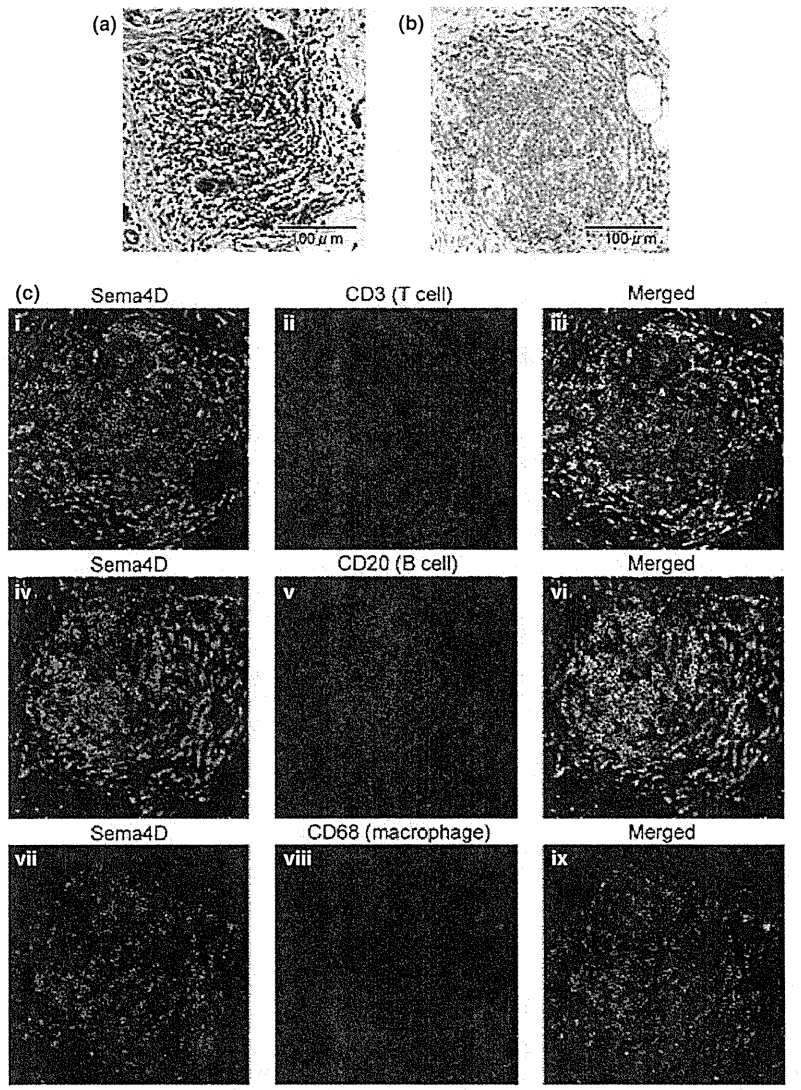

Fig. 2. Semaphorin 4D (Sema4D) expression in human pancreatic cancer tissues. (a) Hematoxylin–eosin staining of Sema4D-expressing cells. (b) Immunohistochemistry for Sema4D. (c) Immunofluorescent staining demonstrated that Sema4D staining largely coincided with the staining for the T-cell and B-cell markers in the tumor area. In contrast, Sema4D staining hardly coincided with the staining for the macrophage marker.

Materials and Methods

Tissue sample collection. Ninety-nine paraffin-embedded tissue sections and 11 of pancreatic ductal adenocarcinoma were obtained from the Yokohama City University Hospital (Yokohama, Japan) (for details, see Data S1).

Cell lines, cultures, and reagents. Human pancreatic cancer cell lines were obtained from the American Type Culture Collection (Manassas, VA, USA) and RIKEN Bioresource Center (Ibaraki, Japan), and maintained in the appropriate media containing 10% fetal bovine serum at 37°C in a humidified atmosphere containing 5% CO_2. Human pancreatic duct epithelial (HPDE) cells were cultured in keratinocyte serum-free medium supplemented with bovine pituitary extract and epidermal growth factor (for details about reagents, see Data S1).

RNA extraction and real-time quantitative PCR. Total RNA from the frozen tissues was extracted using ISOGEN (Nippon-Gene, Tokyo, Japan), according to the manufacturer's instructions. After the cDNA was synthesized, real-time quantitative PCR was performed with an iCycler and *Taq*Man Gene Expression Master Mix (Applied Biosystems, Carlsbad, CA, USA) (for details, see Data S1).

Immunohistochemical studies. Immunohistochemical studies were performed in a standard protocol (for details, see Data S1).

Immunohistochemistry scoring. Three investigators, including a board-certified pathologist, independently assessed the stained sections. We counted total infiltrating inflammatory cells in the cancer stroma in 10 independent high-power (×400) microscopic fields for each tissue sample. The percentage of Sema4D-positive cells was also assessed against total inflammatory cells. The degree of positivity was classified into three grades: grade 1, 0–25%, positive; grade 2, 26–50%, positive; and grade 3, 51–100%, positive. For the statistical analyses, grades 1 and 2 were defined as low expression, and grade 3 was defined as high expression. The expression level of plexinB1 in the cancer cells of each patient was compared to that in the pancreatic ductal

Table 1. Correlations of the clinicopathological features with the expressions of semaphorin 4D (Sema4D) and plexinB1

Characteristics	Sema4D expression, *n* (%)			PlexinB1 expression, *n* (%)		
	Low (*n* = 52)	High (*n* = 47)	*P*-value	Low (*n* = 54)	High (*n* = 45)	*P*-value
Age (years)						
≥60	37 (71.2)	39 (83.0)	0.16	41 (75.9)	35 (77.8)	0.83
<60	15 (28.8)	8 (17.0)		13 (24.1)	10 (22.2)	
Sex						
Male	28 (53.8)	31 (66.0)	0.22	33 (61.1)	26 (57.8)	0.74
Female	24 (46.2)	16 (34.0)		21 (38.9)	19 (42.2)	
Pathological tumor status†						
pT1	2 (3.8)	0 (0.0)	0.054	1 (1.9)	1 (2.2)	0.24
pT2	2 (3.8)	0 (0.0)		0 (0.0)	2 (4.4)	
pT3	48 (92.3)	47 (100.0)		53 (98.1)	42 (93.3)	
pT4	0 (0.0)	0 (0.0)		0 (0.0)	0 (0.0)	
Pathological node status†						
pN0	14 (26.9)	3 (6.4)	0.0068*	12 (22.2)	5 (11.1)	0.14
pN1	38 (73.1)	44 (93.6)		42 (77.8)	40 (88.9)	
Pathological metastasis status†						
pM0	47 (90.4)	35 (74.5)	0.036	50 (92.6)	32 (71.1)	0.0048*
pM1	5 (9.6)	12 (25.5)		4 (7.4)	13 (28.9)	
Stage†						
Ia	1 (1.9)	0 (0.0)	0.0020*	0 (0.0)	1 (2.2)	0.0072*
Ib	0 (0.0)	0 (0.0)		0 (0.0)	0 (0.0)	
IIa	13 (25.0)	3 (6.4)		12 (22.2)	4 (8.9)	
IIb	33 (63.5)	32 (68.1)		38 (70.4)	27 (60.0)	
III	0 (0.0)	0 (0.0)		0 (0.0)	0 (0.0)	
IV	5 (9.6)	12 (25.5)		4 (7.4)	13 (28.9)	
Tumor grade						
Grade 1‡	12 (23.1)	12 (25.5)	0.51	11 (20.4)	13 (28.9)	0.83
Grade 2‡	36 (69.2)	26 (55.3)		39 (72.2)	23 (51.1)	
Grade 3‡	4 (7.7)	9 (19.1)		4 (7.4)	9 (20.0)	
Lymphatic invasion§						
Negative	18 (34.6)	12 (25.5)	0.33	20 (37.0)	10 (22.2)	0.11
Positive	34 (65.4)	35 (74.5)		34 (63.0)	35 (77.8)	
Venous invasion§						
Negative	17 (32.7)	6 (12.8)	0.019*	16 (29.6)	7 (15.6)	0.099
Positive	35 (67.3)	41 (87.2)		38 (70.4)	38 (84.4)	
Extrapancreatic nerve plexus invasion§						
Negative	35 (67.3)	19 (40.4)	0.0073*	31 (57.4)	23 (51.1)	0.53
Positive	17 (32.7)	28 (59.6)		23 (42.6)	22 (48.9)	

*$P < 0.05$. †Classified according to the International Union Against Cancer tumor-node-metastasis classification.[20] ‡Classified according to the World Health Organization classification.[22] §Classified according to the classification of pancreatic carcinoma of Japan Pancreas Society.[21]

epithelial cells in non-tumor area from the same patient, and scored in comparison with the staining intensity in the ductal epithelial cells: 0, no staining; 1, weak staining intensity compared to the pancreatic ductal epithelial cells in the non-tumor area; 2, moderate staining intensity; and 3, strong staining intensity. The cut-off value between scores 1 and 2 is whether the staining intensity is stronger than that of the pancreatic ductal epithelial cells in the non-tumor area in the same patient. Finally, the score that defined the largest area was determined as the score for each specimen. For the statistical analyses, a score of 0 or 1 was defined as low expression, and a score of 2 or 3 was defined as high expression.

Western blot analysis. Cell lysates were prepared and subjected to Western blot analysis (for details, see Data S1).

Cell growth assay. Cell growth assay was performed using CellTiter-Blue reagent (Promega, Madison, WI, USA), according to the manufacturer's instructions (for details, see Data S1).

Cell invasiveness assay. The cell invasiveness assay was performed using BioCoat Matrigel Invasion Chambers (BD Biosciences, San Jose, CA, USA), according to the manufacturer's instructions (for details, see Data S1).

Generation of stable transfectant-induced siRNA for plexin B1. The vector encoding the shRNA sequence for plexin B1 RNAi and the control vector was purchased from SA Biosciences (Frederick, MD, USA). Each of the vectors was transfected into PANC-1 cells and PK-1 cells by electroporation using Nucleofector II (Amaxa, Gaithersburg, MD, USA). The transfected cells were selected by G418 (800 μg/mL) over a 3-week period. After the specific downregulation of plexinB1 was confirmed by Western blotting, the cells were used for further experiments.

Ras homolog gene family, member A activation assay. The RhoA activation assay was performed using the G-LISA RhoA activation assay kit (Cytoskeleton, Denver, CO, USA), according to the manufacturer's instructions (for details, see Data S1).

Statistical analyses. All statistical analyses were performed using SPSS for Windows (SPSS, Chicago, IL, USA) (for details, see Data S1).

Results

Semaphorin 4D and plexin B1 mRNA overexpression in pancreatic cancer tissues. To investigate the Sema4D expression status in pancreatic cancer, we evaluated the expressions of Sema4D and plexinB1 at the mRNA level in 11 human pancreatic cancer tissue specimens. Quantitative real-time PCR

doi: 10.1111/j.1349-7006.2011.02053.x

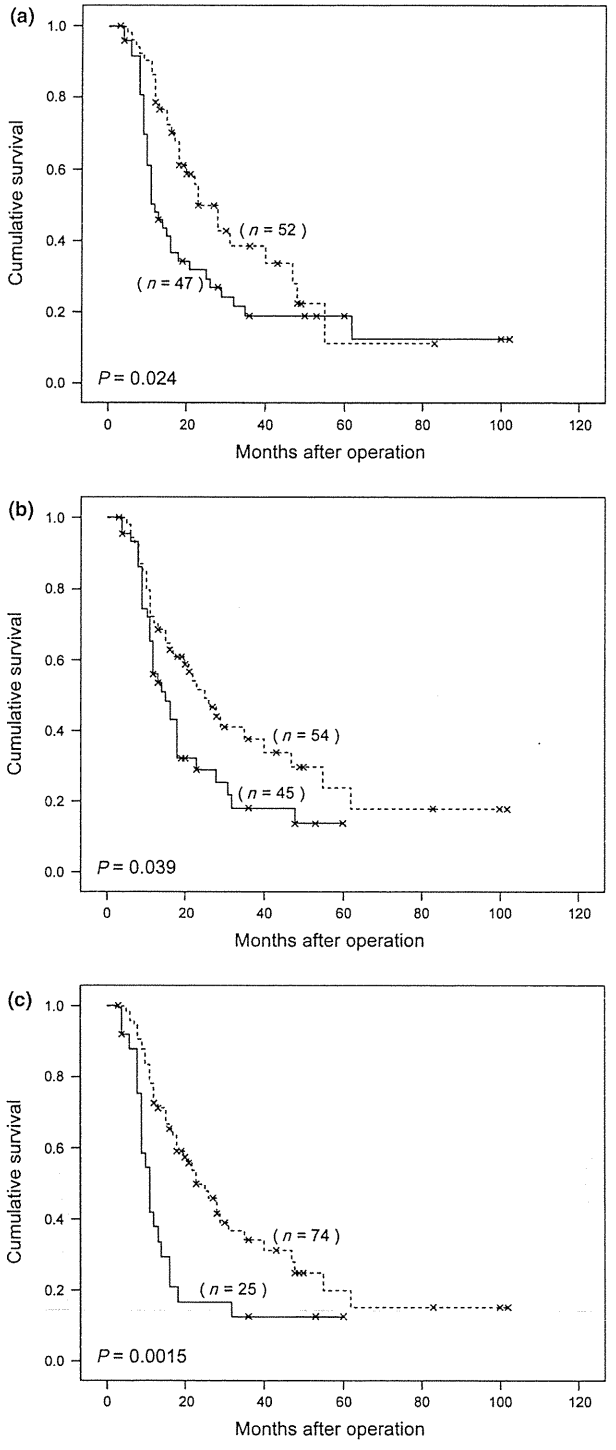

Fig. 3. Prognostic significance of Semaphorin 4D (Sema4D) and plexinB1 expressions. (a) Group showing high Sema4D expression levels showed worse survival than the group with tumors showing low Sema4D expression levels ($P = 0.024$). High expression of Sema4D (-x-) and low expression of Sema4D (··x··). (b) Group showing high plexinB1 expression levels also showed worse survival than the group showing low plexinB1 expression levels ($P = 0.039$). High expression of plexinB1 (-x-) and low expression of plexinB1 (··x··). (c) Group showing high expression levels of both Sema4D and plexinB1 showed significantly worse survival than all the other groups ($P = 0.0015$). High expression of Sema4D and plexinB1 (-x-) and others (··x··).

analyses revealed that both Sema4D and plexinB1 mRNA were significantly overexpressed in the pancreatic cancer tissues, as compared to the expression levels in the paired, non-tumor pancreatic tissues obtained from the same patients ($P = 0.0034$, $P = 0.0059$, respectively) (Fig. 1a).

Semaphorin 4D expression in cancer stromal tissues. An imunohistochemical analysis of the 99 pancreatic cancer specimens revealed that the expression of Sema4D was not detected in the cancer cells, but in the cancer stroma (Fig. 1b). The strong expression of plexinB1 was observed in the cancer epithelial cells, whereas only faint expression was seen in the pancreatic ductal epithelial cells in the non-tumor area (Fig. 1c). Additional double-immunofluorescent staining demonstrated that the Sema4D staining largely coincided with the staining for the T-cell and B-cell markers, but hardly coincided with that for the macrophage marker (Fig. 2c; hematoxylin–eosin staining and immunohistochemistry for Sema4D of the same sample were also shown in Figure 2a,b, respectively).

Correlations of the clinicopathological features with the expressions of Sema4D and plexinB1. For the sake of simplicity, while evaluating the correlation between the Sema4D expression and the clinicopathological features, the 99 samples were divided into 52 samples showing 0–50% positivity, and 47 showing 51–100% positivity for Sema4D expression. Increased Sema4D expression was significantly correlated with the presence of lymph node metastasis ($P = 0.0068$), presence of distant metastasis ($P = 0.036$), advanced stage of the tumor ($P = 0.0020$), venous invasion ($P = 0.019$), and extrapancreatic nerve plexus invasion ($P = 0.0073$) (Table 1). For a similar evaluation of plexinB1 expression, the 99 specimens were divided into 54 samples with a score of 0 or 1, and 45 with a score of 2 or 3 for plexinB1 expression. Increased plexinB1 expression was significantly correlated with the presence of distant metastasis ($P = 0.0048$) and an advanced stage of the disease ($P = 0.0072$).

Prognostic significance of Sema4D/plexinB1 expression. In the analysis of overall survival, the overall median survival of the patients was 18.3 months. The group showing low Sema4D expression levels showed better survival than the group showing high Sema4D expression levels ($P = 0.024$, Fig. 3a). Similarly, in the case of plexinB1, increased expression was correlated with a worse survival ($P = 0.039$; Fig. 3b). When the expressions of both Sema4D and plexinB1 were combined to analyze their additive effect on survival, the mean survival was significantly shorter in the 25 patients showing high expression levels of both Sema4D and plexinB1 (11.7 months), as compared to those in the other groups (23.5 months, $P = 0.0015$, Fig. 3c).

Furthermore, in a univariate analysis performed to compare the significance of Sema4D and plexinB1 expressions with that of the standard parameters, as shown in Table 2, increased Sema4D plus plexinB1 expression was identified as having the second highest prognostic significance ($P = 0.0027$) after distant metastasis ($P = 0.00054$). Finally, in a stepwise multivariable Cox regression model with all standard parameters, only increased Sema4D plus plexinB1 expression ($P = 0.045$), distant metastasis ($P = 0.0018$), and the tumor growth pattern ($P = 0.043$) were identified as significant factors affecting prognosis in all patients (Table 2). The hazard ratio for prognosis was 1.75 for patients showing high expression levels of Sema4D and plexinB1 relative to that in the other patients.

Expression of plexinB1 in pancreatic cancer cell lines. The observed correlations between the clinicopathological features and Sema4D/plexinB1 expressions in the pancreatic cancer tissue samples prompted us to clarify the function of the Sema4D-plexinB1 signaling pathway in the pancreatic cancer cell lines. In the Western blot analysis, the band corresponding to plexinB1 was detected in all the pancreatic cancer cell lines examined,

Table 2. Hazard ratios (HR) of clinicopathological characteristics determined for overall survival

Univariate analysis		Overall survival	
Variables	Categories	HR (95% CI)	*P*-value
Semaphorin 4D and plexinB1 expression	Both high level versus others	2.25 (1.33–3.80)	0.0024*
Age (years)	<60 *vs* ≥60	1.20 (0.68–2.11)	0.53
Sex	Male versus female	1.61 (0.98–2.70)	0.063
Pathological tumor status	pT1 + pT2 versus pT3	3.89 (0.54–28.10)	0.18
Pathological node status	pN0 versus pN1	1.63 (0.80–3.29)	0.18
Pathological metastasis status	pM0 versus pM1	2.81 (1.57–5.06)	0.00054*
Tumor grade	Grade 1 versus grades 2 + 3	1.07 (0.61–1.88)	0.82
Tumor size (cm)	≤2.0 *vs* >2.0	2.27 (1.04–4.99)	0.041*
Growth pattern	Expansive + intermediate versus infiltrative	1.67 (1.01–2.75)	0.046*
Chemoradiotherapy	Received versus not received	0.661 (0.36–1.21)	0.18
Multivariate analysis			
Semaphorin 4D and plexinB1 expression	Both high level versus others	1.75 (1.01–3.02)	0.045*
Pathological metastasis status	pM0 versus pM1	2.65 (1.44–4.88)	0.0018*
Growth pattern	Expansive + intermediate versus infiltrative	1.70 (1.02–2.83)	0.043*

Chi-square test model result was significant ($P < 0.001$). *$P < 0.05$. CI, confidence interval.

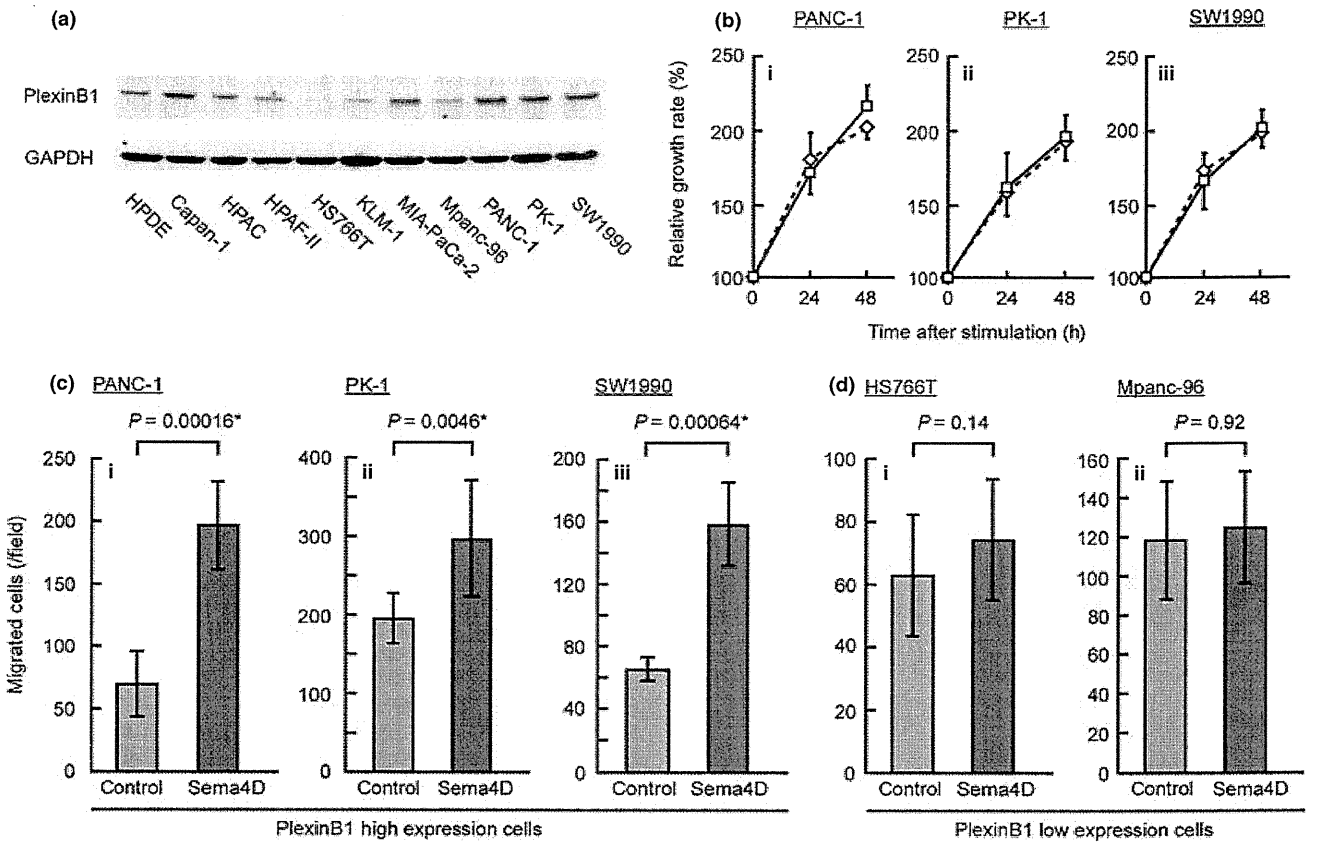

Fig. 4. Semaphorin 4D (Sema4D) augmented the invasive potential of the tumor cells in the pancreatic cancer cell lines. (a) Western blot analysis revealed endogenous plexinB1 expression in all the pancreatic cancer cell lines examined, although at varying expression levels. (b) Semaphorin 4D stimulation failed to enhance the cell growth in the pancreatic cancer cell lines expressing endogenous plexinB1. Control (-◇-) and Sema4D (-□-). (c) Semaphorin 4D stimulation significantly enhanced the invasive potential of cells showing high expression levels of plexinB1 (PANC-1, $P = 0.00016$; PK-1, $P = 0.0046$; SW1990, $P = 0.00064$, respectively). (d) Semaphorin 4D stimulation failed to augment the invasive potential of the cells, showing low expression levels of plexinB1 (HS766T, $P = 0.14$, Mpanc-96, $P = 0.92$, respectively). HPDE, human pancreatic duct epithelial cells.

although the expression levels varied among the cell lines (Fig. 4a). Capan-1, MIAPaCa-2, PANC-1, PK-1, and SW1990 showed higher expression levels than normal HPDE cells.

Semaphorin 4D augmentation of the invasive potential of tumor cells in pancreatic cancer cell lines. To evaluate the function of the Sema4D/plexinB1 signaling pathway in the

doi: 10.1111/j.1349-7006.2011.02053.x

pancreatic cancer cell lines, we evaluated whether exogenous Sema4D stimulation could activate cancer cell growth or potentiate cellular invasive activity. Using three pancreatic cancer cell lines that are known to show high endogenous expression levels of plexinB1 (PANC-1, PK-1, and SW1990), the effect of Sema4D stimulation on the cell growth rate was evaluated. However, this experiment showed the absence of any significant differences in the cell growth rate between the Sema4D-stimulated cells and the control cells (Fig. 4b).

The cellular invasive activity was strongly induced by Sema4D stimulation. The invasive activity was evaluated using Transwell chambers. The migrated cell number was significantly higher in the Sema4D-stimulated wells than in the control wells (PANC-1, $P = 0.00016$; PK-1, $P = 0.0046$; SW1990, $P = 0.00064$, respectively, Fig. 4c). The same experiments were performed with two other pancreatic cancer cell lines that showed low endogenous expression levels of plexinB1 (HS766T and Mpanc-96); Sema4D stimulation failed to increase the invasiveness of these cells (HS766T, $P = 0.14$; Mpanc-96, $P = 0.92$, Fig. 4d).

To confirm the role of plexinB1 in Sema4D stimulation, we introduced an siRNA for plexinB1 into the PANC-1 and PK-1 cells and established a mixture of cell lines expressing siRNA for plexinB1, as well as vector control cells. As shown in Figure 5a, we confirmed the reduced expression of plexinB1 in the pooled transfectants, as compared to that in the control cells by Western blotting. The results of the invasiveness assay using these cells were as expected. Semaphorin 4D failed to potentiate the cellular invasiveness in the plexinB1 siRNA-transfected cells (Fig. 5b). These findings confirmed that the effect of Sema4D stimulation in potentiating the invasiveness of pancreatic cancer cells was mediated by endogenous plexinB1.

Semaphorin 4D induces the phosphorylation of MAPK and Akt through the activation of Ras homolog gene family, member A. To clarify the regulatory mechanism of cell motility by Sema4D, we examined the two major downstream pathways. One of the potential candidates is the tyrosine kinase receptor Met pathway; however, in our study, the phosphorylation of Met by Sema4D stimulation was not observed (Fig. 6b). Subsequently, we evaluated RhoA activity after the stimulation of Sema4D as the other candidate downstream molecule. The results revealed that Sema4D stimulation could activate RhoA within a very short time (Fig. 6a). In addition, Sema4D could induce the phosphorylation of Akt and MAPK, which are downstream molecules in the plexinB1/RhoA pathway, as previously demonstrated (Fig. 6b). We confirmed that Sema4D could not activate RhoA or its downstream molecules in plexinB1 knockdown cell lines (Fig. 6c,d). These findings indicate that the Sema4D signal is transmitted directly downstream of plexinB1 through the activation of RhoA.

Discussion

In this study, we report our identification of a new signaling pathway, the activation of which can enhance the tumor cell motility in pancreatic cancer. We demonstrated that the overexpression of Sema4D and its receptor plexinB1 were significantly correlated with clinical factors, such as lymph node metastasis and distant metastasis, in patients with PDAC. Because the expressions of these molecules reflect the tumor invasive and metastatic potentials in human PDAC samples, they were thought to play a role in the regulation of the tumor cell motility in pancreatic cancer.

Through the *in vitro* experiments, we demonstrated that Sema4D can potentiate the invasive ability of the pancreatic cancer cells, and that the Sema4D signaling was mediated by the plexinB1 expressed on the cancer cells. We also identified the downstream molecules in the Sema4D/plexinB1 signaling pathway. The binding of Sema4D to plexinB1 induced RhoA activation within a very short time, and RhoA activation in turn induced the phosphorylation of MAPK and Akt, a response necessary for cell migration.[23] The phosphorylation of the Met protein, the other pathway of Sema4D/plexinB1 signaling mentioned earlier, was not observed in our study.

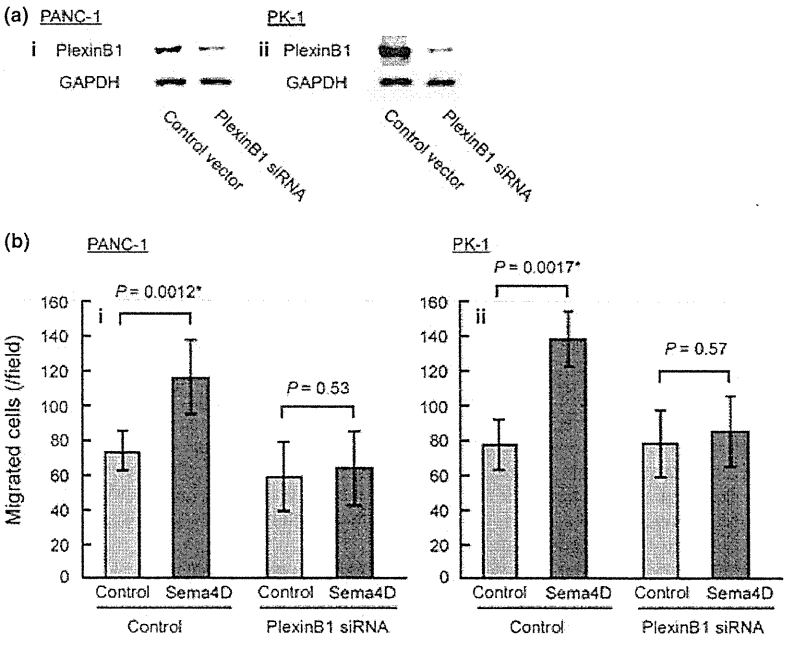

Fig. 5. PlexinB1 knockdown by siRNA. (a) Reduced expression of plexinB1 induced by plexinB1 siRNA was confirmed at the protein level. (b) Induction of cellular invasiveness by semaphorin 4D stimulation was not observed in the plexinB1 knockdown cells.

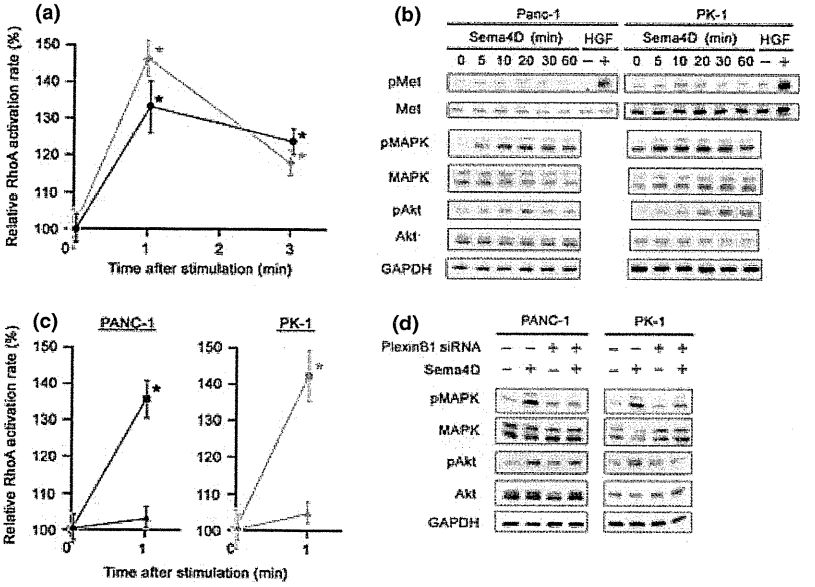

Fig. 6. Downstream molecules in the semaphorin 4D (Sema4D)/plexinB1 signaling pathway. (a) Evaluation of Ras homolog gene family, member A (RhoA) activity after Sema4D stimulation. Results revealed that Sema4D could activate RhoA within a very short time (*$P < 0.05$). PANC-1 (–●–) and PK-1 (–◈–). (b) Time course of Met, MAPK, and Akt activation downstream of the Sema4D/plexinB1 signaling pathway. Each cell line was treated with 8 nM Sema4D for the time period indicated. Activation of Met induced by Sema4D was not observed. For the positive control, we used the samples treated with 25 ng/mL hepatocyte growth factor (HGF) for 15 min. Activation of both MAPK and Akt was observed from 5 min after the start of Sema4D stimulation and peaked at 20 min. (c) Semaphorin 4D could not enhance the activity of Ras homolog gene family, member A (RhoA) in the plexinB1 knockdown cells. After 1-min stimulation, Sema4D could also activate RhoA in the control cells, but not in the plexinB1 knockdown cells (*$P < 0.05$). Control (–■–) (–▫–) and plexinB1 siRNA (–▲–) (–△–). (d) Semaphorin 4D could not induce MAPK or Akt activation in the plexinB1 knockdown cells. According to the results of the time course analysis, each cell line was treated with 8 nM Sema4D or serum-free medium for 20 min.

For potential therapeutic application, it is important to assess whether we can inhibit this signaling pathway. We clearly demonstrated that plexinB1 knockdown by siRNA could inhibit the Sema4D signal transmitted to the downstream molecules. Although further analyses, including *in vivo* experiments, are needed to validate the finding that knockdown of plexinB1 can indeed suppress the invasive activity of pancreatic cancer cells, these molecules are nonetheless promising candidates as therapeutic targets in patients with PDAC.

Because Sema4D and plexinB1 expressions reflect the invasive and metastatic potentials of tumor cells, it would be reasonable to assume that they might be correlated with the prognosis of PDAC patients. We also demonstrated the prognostic impact of Sema4D and plexinB1 expressions in this study. The multivariable analysis revealed that the increased expression of both Sema4D and plexinB1 was associated with an additive worsening of the prognosis, independent of the TNM classification and World Health Organization tumor grade. Because of the dismal survival rate, the determination of prognostic factors that would allow identification of patients who can potentially benefit from aggressive treatment is important for patients with pancreatic cancer. However, to date, there have been no established prognostic factors in pancreatic cancer patients whose usefulness has been proven by at least two examinations.[24] Further studies are necessary to confirm the actual clinical usefulness of these molecules; however, Sema4D and plexinB1 are considered to offer strong potential as candidate tumor markers.

In the tumor microenvironment, the Sema4D protein can be produced by many kinds of cells.[6] The expression of Sema4D in human cancer tissues has been reported in only one previous article;[25] that article reported the expression of Sema4D on both cancer cells and the tumor-infiltrating lymphocytes in a human soft tissue sarcoma. In addition, it has been reported that the main cells producing Sema4D in the tumor stroma in breast cancer were tumor-associated macrophages.[19] In the present study, we revealed for the first time that the cells expressing Sema4D in the tumor stroma in human pancreatic cancer were tumor-infiltrating lymphocytes. We could obtain only limited evidence about the predominant cells producing Sema4D in the tumor stroma; however, we believe that the tumor-infiltrating lymphocytes are certainly one of the candidate cells showing Sema4D expression within the tumor stroma.

In conclusion, we demonstrated a new signaling pathway that can contribute to enhanced tumor cell motility in pancreatic cancer. As many attempts are now ongoing to target the molecules associated with the invasive and metastatic potential of cancer cells, we propose Sema4D/plexinB1 as a new target for pancreatic cancer therapy.

Acknowledgments

This work was supported in part by a Grant-in-Aid for research on the Third Term Comprehensive Control Research for Cancer from the Ministry on Health, Labor and Welfare, Japan, to AN, and a grant from Yokohama Foundation for Advancement Medical Science.

Disclosure Statement

Shingo Kato received a research grant from Yokohama Foundation for Advancement Medical Science. Atsushi Nakajima received a research grant from the Ministry on Health, Labor and Welfare, Japan.

doi: 10.1111/j.1349-7006.2011.02053.x

References

1 Jemal A, Siegel R, Xu J, Ward E. Cancer statistics, 2010. *CA Cancer J Clin* 2010; **60**: 277–300.
2 Tanaka T, Ikeda M, Okusaka T *et al.* Prognostic factors in japanese patients with advanced pancreatic cancer treated with single-agent gemcitabine as first-line therapy. *Jpn J Clin Oncol* 2008; **38**: 755–61.
3 Li D, Xie K, Wolff R, Abbruzzese JL. Pancreatic cancer. *Lancet* 2004; **363**: 1049–57.
4 Pasterkamp RJ, Kolodkin AL. Semaphorin junction: making tracks toward neural connectivity. *Curr Opin Neurobiol* 2003; **13**: 79–89.
5 Kolodkin AL, Matthes DJ, Goodman CS. The semaphorin genes encode a family of transmembrane and secreted growth cone guidance molecules. *Cell* 1993; **75**: 1389–99.
6 Bismuth G, Boumsell L. Controlling the immune system through semaphorins. *Sci STKE* 2002; **128**: re4.
7 Kikutani H, Kumanogoh A. Semaphorins in interactions between T cells and antigen presenting cells. *Nat Rev Immunol* 2003; **3**: 159–67.
8 Giordano S, Corso S, Conrotto P *et al.* The semaphorin 4D receptor controls invasive growth by coupling with Met. *Nat Cell Biol* 2002; **4**: 720–4.
9 Tse C, Xiang RH, Bracht T, Naylor SL. Human Semaphorin 3B (SEMA3B) located at chromosome 3p21.3 suppresses tumor formation in an adenocarcinoma cell line. *Cancer Res* 2002; **62**: 542–6.
10 Christensen CR, Klingelhöfer J, Tarabykina S, Hulgaard EF, Kramerov D, Lukanidin E. Transcription of a novel mouse semaphoring gene, M-semaH, correlates with the metastatic ability of mouse tumor cell lines. *Cancer Res* 1998; **58**: 1238–44.
11 Boumsell L, Schmid M, Dastot H, Gouttefangeas C, Mathieu-Mahul D, Bensussan A. *In vitro* differentiation from a pluripotent human CD4+CD8+ thymic cloned cell into four phenotypically distinct subsets. *J Immunol* 1990; **145**: 2797–802.
12 Bougeret C, Mansur IG, Dastot H *et al.* Increased surface expression of a newly identified 150-kDa dimer early after human T lymphocyte activation. *J Immunol* 1992; **148**: 318–23.
13 Hall KT, Boumsell L, Schultze JL *et al.* Human CD100, a novel leukocyte semaphorin that promotes B-cell aggregation and differentiation. *Proc Natl Acad Sci USA* 1996; **93**: 11780–5.
14 Kumanogoh A, Watanabe C, Lee I *et al.* Identification of CD72 as a lymphocyte receptor for the class IV semaphorin CD100: a novel mechanism for regulating B cell signaling. *Immunity* 2000; **13**: 621–31.
15 Tamagnone L, Artigiani S, Chen H *et al.* Plexins are a large family of receptors for transmembrane, secreted, and GPI anchored semaphorins in vertebrates. *Cell* 1999; **99**: 71–80.
16 Gentile A, Trusolino L, Comoglio PM. The Met tyrosine kinase receptor in development and cancer. *Cancer Metastasis Rev* 2008; **27**: 85–94.
17 Basile JR, Barac A, Zhu T, Guan KL, Gutkind JS. Class IV semaphorins promote angiogenesis by stimulating Rho-initiated pathways through plexin-B. *Cancer Res* 2004; **64**: 5212–24.
18 Basile JR, Gavard J, Gutkind JS. Plexin-B1 utilizes RhoA and Rho kinase to promote the integrin-dependent activation of Akt and ERK and endothelial cell motility. *J Biol Chem* 2007; **282**: 34888–95.
19 Sierra JR, Corso S, Caione L *et al.* Tumor angiogenesis and progression are enhanced by Sema4D produced by tumor-associated macrophages. *J Exp Med* 2008; **205**: 1673–85.
20 Hermanek P, Hutter RVP, Sobin LH, Wagner G, Wittekind CH. *TNM Atlas*, 4th edn. Berlin: SpringerVerlag, 1997; 144–53.
21 Japan Pancreas Society. *Classification of Pancreatic Carcinoma*, (English Edition). Tokyo: Kanehara, 1998; 39.
22 Kloppel G, Hruban RH, Longnecker DS, Adler G, Kern SE, Partanen TJ. Ductal adenocarcinoma of the pancreas. In: Hamilton SR, Aaltonen LA, eds. *Pathology and Genetics. Tumours of the Digestive System.* WHO classification of tumours. Lyon: IARC Press, 2000; 220–30.
23 Basile JR, Afkhami T, Gutkind JS. Semaphorin 4D/plexin-B1 induces endothelial cell migration through the activation of PYK2, Src, and the phosphatidylinositol 3-kinase-Akt pathway. *Mol Cell Biol* 2005; **25**: 6889–98.
24 Tonini G, Pantano F, Vincenzi B, Gabbrielli A, Coppola R, Santini D. Molecular prognostic factors in patients with pancreatic cancer. *Expert Opin Ther Targets* 2007; **11**: 1553–69.
25 Ch'ng E, Tomita Y, Zhang B *et al.* Prognostic significance of CD100 expression in soft tissue sarcoma. *Cancer* 2007; **110**: 164–72.

Supporting Information

Additional Supporting Information may be found in the online version of this article:

Data S1. Materials and methods.

Please note: Wiley-Blackwell are not responsible for the content or functionality of any supporting materials supplied by the authors. Any queries (other than missing material) should be directed to the corresponding author for the article.

Published OnlineFirst May 12, 2011; DOI:10.1158/0008-5472.CAN-10-2475

Cancer Research

Tumor Suppressor *miR-22* Determines p53-Dependent Cellular Fate through Post-transcriptional Regulation of p21

Naoto Tsuchiya, Masashi Izumiya, Hiroko Ogata-Kawata, et al.

Cancer Res 2011;71:4628-4639. Published OnlineFirst May 12, 2011.

Published OnlineFirst May 12, 2011; DOI:10.1158/0008-5472.CAN-10-2475

Tumor and Stem Cell Biology

Cancer Research

Tumor Suppressor *miR-22* Determines p53-Dependent Cellular Fate through Post-transcriptional Regulation of p21

Naoto Tsuchiya[1], Masashi Izumiya[1], Hiroko Ogata-Kawata[1], Koji Okamoto[2], Yuko Fujiwara[1], Makiko Nakai[1], Atsushi Okabe[3], Aaron J. Schetter[5], Elise D. Bowman[5], Yutaka Midorikawa[4], Yasuyuki Sugiyama[4], Hiroyuki Aburatani[3], Curtis C. Harris[5], and Hitoshi Nakagama[1]

Abstract

Selective activation of p53 target genes in response to various cellular stresses is a critical step in determining the ability to induce cell-cycle arrest or apoptosis. Here we report the identification of the microRNA *miR-22* as a p53 target gene that selectively determines the induction of p53-dependent apoptosis by repressing p21. Combinatorial analyses of the AGO2 immunocomplex and gene expression profiles identified *p21* as a direct target of *miR-22*. Induction of p21 was inhibited by *miR-22* after exposure to the genotoxic agent Adriamycin (doxorubicin; Bedford Laboratories), sensitizing cells to p53-dependent apoptosis. Interestingly, the activation of *miR-22* depended on the intensity of the stresses that induced cells to undergo apoptosis in the presence of *p21* suppression. Our findings define an intrinsic molecular switch that determines p53-dependent cellular fate through post-transcriptional regulation of p21. *Cancer Res; 71(13); 4628–39. ©2011 AACR.*

Introduction

The p53 tumor suppressor network plays a crucial role in the prevention of malignant transformation in normal cells by maintaining the integrity of signaling pathways in response to various oncogenic stresses, including DNA damage, acute activation of oncogenes, and hypoxic conditions (1). The outcome of p53 activation in response to cellular stresses ranges from the induction of cell-cycle arrest for DNA repair to apoptosis for the complete elimination of damaged cells (2–4). The commitment to one of these alternative cellular fates depends on the set of p53 target genes induced by different stresses. Induction of cell-cycle arrest is mediated by the activation of the cyclin-dependent kinase inhibitor *CDKN1A* (hereafter referred to as p21), whereas apoptosis is induced by the activation of pro-apoptotic genes, including *NOXA* (5), *PUMA* (6), and *BAX* (7) that encode the regulators of intrinsic apoptosis pathways.

Authors' Affiliations: Divisions of [1]Cancer Development System and [2]Cancer Differentiation, National Cancer Center Research Institute, Tsukiji; [3]Genome Science Division, Research Center for Advanced Science and Technology, The University of Tokyo, Komaba, Tokyo; [4]Teikyo University School of Medicine, University Hospital, Mizonokuchi, Kawasaki-shi, Kanagawa, Japan; and [5]Laboratory of Human Carcinogenesis, Center for Cancer Research, National Cancer Institute, National Institute of Health, Bethesda, Maryland

Note: Supplementary data for this article are available at Cancer Research Online (http://cancerres.aacrjournals.org/).

Corresponding Author: Hitoshi Nakagama, National Cancer Center Research Institute, 1-1 Tsukiji 5-chome, Tokyo 104-0045, Japan. Phone: 81-3-3547-5242; Fax: 81-3-3547-5242; E-mail: hnakagam@ncc.go.jp

doi: 10.1158/0008-5472.CAN-10-2475

Post-translational modifications of p53 are involved in the selective activation of its various target genes leading to apoptosis (8, 9). Phosphorylation of p53 at serine 46 (Ser46), mediated by HIPK2 (10), regulates apoptotic pathways through the activation of *p53AIP1* (11). Furthermore, acetylation of p53 at lysine 120 (K120) by Tip60 is essential for the expression of *PUMA* (12). Ongoing work focuses on the elucidation of p53 function and its regulation as a transcriptional factor.

Recently, the regulation of gene expression by small noncoding RNAs, including microRNAs (miRNA), has been reported to play crucial roles in the maintenance of homeostasis in a wide range of cellular processes, including differentiation, control of cell proliferation, and stress responses (13–15). The important feature of miRNAs is the targeting of multiple cellular mRNAs, resulting in the efficient activation or repression of intracellular or intercellular signaling networks at specific times during animal development. miRNA dysfunction therefore causes defects in the integration of signaling networks essential for the maintenance of cellular homeostasis.

miRNA dysfunction has been suggested as a dominant cause of the onset of human disorders, especially cancers. Indeed, aberrant expression of miRNA genes was observed in almost all types of human cancers (16, 17). As a consequence of miRNA dysfunction, cancer cells acquire properties that favor the activation of oncogenic pathways or the repression of tumor-suppressive networks, contributing to cancer progression and metastasis (18–22). *MiR-21* was shown to repress *PTEN*, activating the phosphoinositide 3-kinase (PI3K)–AKT pathway and reflecting its oncogenic role (23). By contrast, *miR-34a* was identified as a p53-regulated tumor-suppressive miRNA in human colon cancer and shown to induce p53-dependent apoptosis or premature senescence, forming a positive feedback loop with p53 (24–28). The function of miRNAs as oncogenes or tumor suppressor genes is therefore well known, and

Published OnlineFirst May 12, 2011; DOI:10.1158/0008-5472.CAN-10-2475

it implies that the incorporation of miRNA species as critical components of intracellular signaling pathways is crucial for the reconstitution of integrated cancer-related networks necessary to fully clarify the molecular basis of carcinogenesis.

To analyze the connection between miRNAs and signaling networks, a functional genetic screening method named "dropout assay" was recently established using a lentivirus miRNA expression library and a home-made microarray to quickly and efficiently isolate tumor-suppressive miRNAs (29). In the present study, an *in vitro* functional genetic screen and comprehensive genomic screens of clinical samples were used to identify tumor suppressor miRNAs in colon carcinogenesis, with the resulting identification of *miR-22* as a tumor suppressor gene. A p53–*miR-22*–p21 axis was identified as a crucial regulatory component involved in the determination of p53-dependent apoptosis. Our results suggest that *miR-22* is an intrinsic molecular switch or sensor for the determination of p53-dependent cellular fate in response to distinct stresses, and *miR-22* dysfunction could affect the anticancer barrier against various oncogenic insults.

Materials and Methods

Cell culture

HCT 116 (HCT 116 $p53^{+/+}$) and HCT 116 $p53^{-/-}$ (30) were kindly provided by Dr. Bert Vogelstein (The Johns Hopkins University, Baltimore, MD). These cell lines were authenticated by morphologic inspection, and mycoplasma testing using PCR. The activation of p53 pathways was confirmed by checking the induction of p53 target genes after exposure to DNA damage before starting the experiments. The SW480 colon cancer cell line was obtained from the American Type Culture Collection and authenticated as described above. Mutation of *TP53* was confirmed by sequencing. These cell lines were maintained in Dulbecco's Modified Eagle's Medium supplemented with 10% heat inactivated FBS in humidified air with 5% CO_2.

Clinical samples

Paired surgical specimens of primary human colon cancers and surrounding noncancerous colon tissue counterparts were obtained from patients treated at the Teikyo University Hospital (Mizonokuchi, Kanagawa, Japan) with documented informed consent in each case. Institutional review board approval for the analysis of clinical samples was obtained at each institute.

Functional miRNA dropout screening

Functional dropout screening to identify tumor suppressor miRNAs was carried out according to our recent publication (29). HCT 116 cells were transduced with a pooled lentivirus miRNA expression library (SBI) at a multiplicity of infections (MOI) of 3. Cells were incubated in complete medium for 3 days (P1) and subjected to sequential passages every 3 days. After 9 passages, genomic DNA was prepared from P1, P5, and P9 cells and subjected to array CGH analysis using a home-made microarray.

Quantitative real-time PCR

For quantitative expression analysis of miRNAs, total RNAs from colon cancer patients were reverse-transcribed by Multiscribe RT and miRNA-specific miRNA primers (ABI), and quantitative real-time PCR (qRT-PCR) was carried out by using a TaqMan microRNA assay kit (ABI). The comparative cycle threshold (C_t) method was applied to quantify the expression levels of miRNAs. Relative expression levels were calculated by the $2^{-\Delta\Delta Ct}$ method. *U48* small nuclear RNA was used as an internal standard.

Chromatin immunoprecipitation sequencing

HCT 116 cells were treated with 5-fluorouracil (5-FU; 0.375 mmol/L) for 9 hours, and chromatin immunoprecipitation (ChIP) was conducted by using anti-p53, antimonomethylated or antitrimethylated histone H3 K4, or antitrimethylated histone H3 K36 antibodies. ChIP-isolated DNA was subjected to the sequencing using an Illumina platform.

AGO2-IP on ChIP analysis

The AGO2-IP on ChIP assay was carried out according to a previous report with minor modifications (31). In brief, HCT 116 cells stably expressing HA-AGO2 were transfected with either *miR-22* (Pre-miR precursor molecule, Ambion) or miR-NC (Pre-miR miRNA Precursor Molecules Negative Control #2, Ambion) for 24 hours, and immunoprecipitated using anti-HA agarose beads. AGO2-bound RNA was eluted in boiling water, and the Trizol-LS reagent was added to extract total RNAs. AGO2-bound total RNAs were cleaned further using an RNeasy column and subjected to microarray analysis.

Reporter plasmid construction and luciferase assay

Amplification of the 3′ UTR of *p21* mRNA was carried out by PCR from HCT 116 genomic DNA using a primer set (Supplementary Table S1). The DNA fragment was fused to the 3′ end of a *firefly* luciferase reporter gene in a pmirGLO dual luciferase vector (Promega). Site-directed mutagenesis of a *miR-22* target site of *p21* mRNA was carried out by using a PrimeSTAR Max high fidelity DNA polymerase using the pmirGLO-*p21* 3'UTR plasmid as a template. HCT 116 cells, seeded at 5×10^4 cells/mL, were cotransfected with 200 ng of reporter plasmid and 10 nmol/L of either *miR-22* or miR-NC using Lipofectamine 2000. After incubation for 24 hours, luciferase activities were determined by using a dual luciferase assay kit (Promega). Luciferase activity was normalized by *Renilla* luciferase activity as an internal standard.

Immunoblot analysis

Cells were lysed in lysis buffer consisting of 25 mmol/L Tris-HCl (pH7.5), 150 mmol/L NaCl, 1 mmol/L EDTA, 1% Triton X-100, 0.1% SDS and 1× proteinase inhibitor cocktail, and equal concentrations of protein samples were loaded on a 10% to 20% polyacrylamide gradient gel (ATTO). After electrophoresis, proteins were transferred to a PVDF membrane, and immunoblot analysis was conducted by the standard method.

Supplementary information

Supplementary information includes extended Materials and Methods, 8 figures, and 4 tables.

Published OnlineFirst May 12, 2011; DOI:10.1158/0008-5472.CAN-10-2475

Results

Identification of *miR-22* as a candidate tumor suppressor miRNA by functional genetic and comprehensive genomic screens

A screening method for the efficient identification of tumor suppressor miRNAs in colon cancer was established and is depicted in Supplementary Fig. S1A. Tumor suppressor miRNAs were defined as follows; (i) repressor of cell proliferation, (ii) expression in normal colon tissue, (iii) high-frequency loss of their chromosomal positions, and (iv) downregulation in human colon cancers. Following these criteria, a functional genetic screening, namely a "dropout assay," was conducted using a lentivirus miRNA expression library (29) to isolate repressors of cell proliferation in a colon cancer cell line (Supplementary Fig. S1B). HCT 116 cells were transduced with a pooled lentivirus library containing 454 miRNA species and propagated for 3 weeks with sequential passages. Genomic DNA from the first passage (P1), fifth passage (P5), and ninth passage (P9) cell populations was prepared, and copy numbers of each miRNA clone in these cells were compared by array CGH analysis using a home-made microarray (Supplementary Fig. S1B). A total 55 miRNA clones were reproducibly dropped out in a culture time-dependent manner (Supplementary Fig. S1C and Table S2). Among these dropout clones, 24 miRNAs were confirmed for their expression in normal tissue (Supplementary Fig. S1D). Furthermore, we carried out array CGH analysis (aCGH) to examine autosomal copy number aberrations using 24 colon cancer patients and finally identified 6 miRNA clones whose genes show hemizygous deletions in cancers with a high frequency (>30%), as candidates for tumor suppressor gene in colon

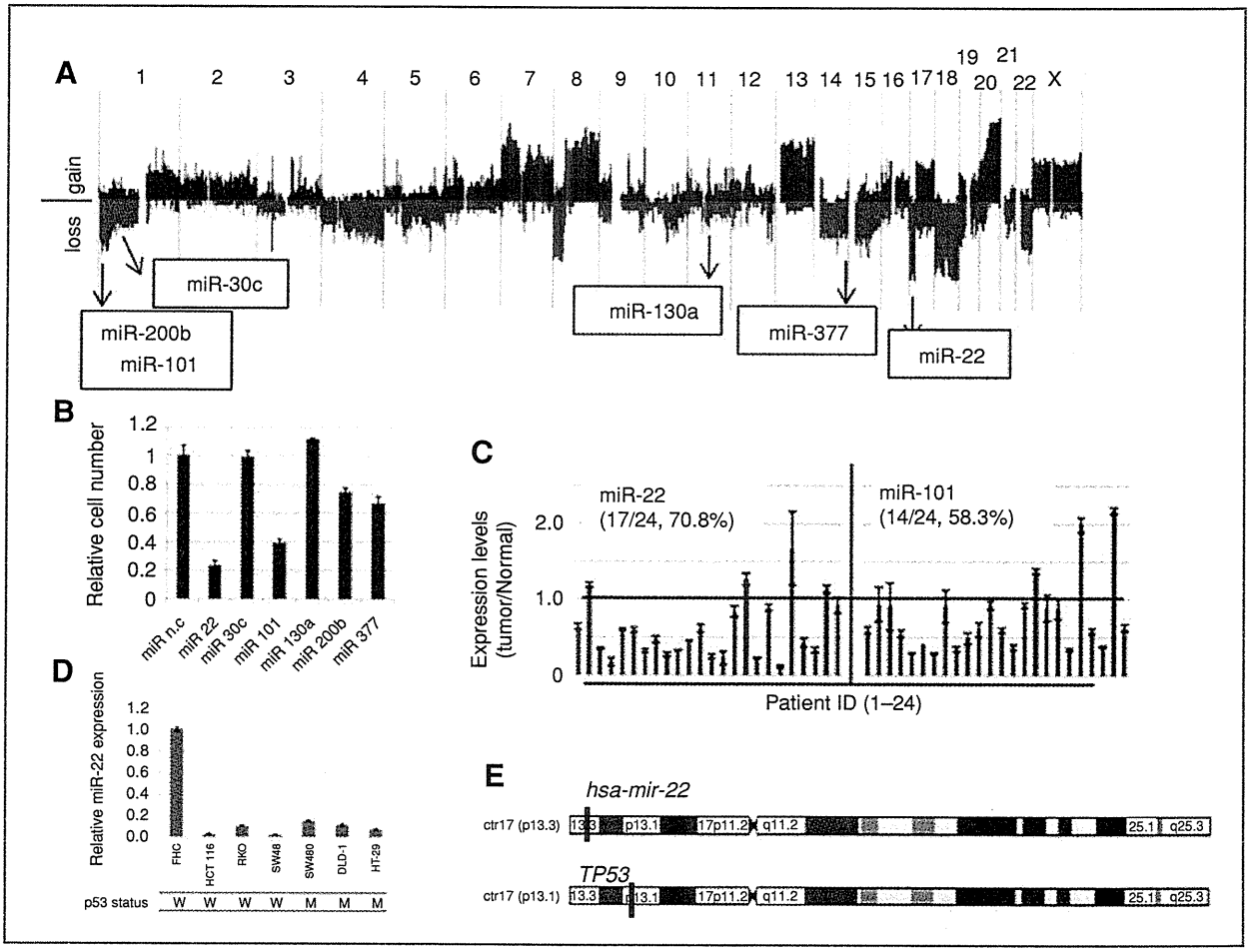

Figure 1. A, result of copy number aberrations in 24 human colon cancer samples. Red and green indicate chromosomal gain and loss, respectively. Chromosomal positions of 6 identified miRNA genes are shown in the CGH result. B, cell proliferation assay. HCT 116 cells were transfected with each synthetic miRNA and incubated for 5 days. Cell viability was measured by MST assay. Error bars indicate SD in triplicate cultures. C, expression of *miR-22* and miR-101 in human colon cancer patients. Expression levels of *miR-22* and *miR-101* were quantified by TaqMan microRNA qRT-PCR. The graphs show the relative expression levels of *miR-22* and *miR-101*, calculated by adjusting their expression levels to matched normal counterparts in each cancer sample. The red line indicates the relative expression level of 1.0. D, expression of *miR-22* in human colon cancer cell lines and normal colon-derived FHC cells. The genomic status of *TP53* in cancer cell lines is indicated. E, chromosomal positions of *miR-22* and *TP53* genes on chromosome 17.

Published OnlineFirst May 12, 2011; DOI:10.1158/0008-5472.CAN-10-2475

Table 1. Genomic status of *hsa-miR-22* and *TP53* genes in 24 human colon cancers

		has-miR-22 (17p13.3)		TP53(17p13.1)					
		chrI7:1,563,947-1,564,081		ChrI7:7,520,037-7,531,588					
Sample No	Patient ID	CNA	Expression (T/N)	CNA	Mutation	Exon	Codon	WT (A.A.)	Mut (A.A.)
1	1002	—	0.635	—	—				
2	1004	—	1.184	—	missense	7	237	ATG (M)	ATA (I)
3	1008	Loss	0.587	Loss	missense	6	193	CAT (H)	CGT(R)
4	1010	Loss	0.172	Loss	missense	8	285	GAG (E)	AAG (K)
5	1011	—	0.602	—	—				
6	1013	Loss	0.001	Loss	—				
7	1014	Loss	0.321	Loss	missense	7	230	GAA (E)	AAA (K)
8	1015	Gain	0.470	Gain	—				
9	1016	Loss	0.272	Loss	insertion (4)	7	280		
10	1017	Loss	0.327	—	—				
11	1018	Loss	0.455	—	—				
12	1019	—	0.614	—	—				
13	1022	Loss	0.248	Loss	missense	7	245	GGC (G)	TGC (C)
14	1023	Loss	0.227	Loss	missense	7	245	GGC (G)	TGC (C)
15	1024	Loss	0.835	Loss	missense	7	248	CGG (R)	CAG (Q)
16	1025	Loss	1.285	Loss	missense	5	175	CGC (R)	CAC (H)
17	1027	Loss	0.227	Loss	missense	7	248	CGG (R)	CAG (Q)
18	1028	Loss	0.888	Loss	missense	5	158	CGC (R)	CAC (H)
19	1029	Loss	0.114	Loss	—				
20	1033	Loss	1.668	Loss	deletion (1)	8	267		
21	1035	Loss	0.429	Loss	deletion (18)	5	174		
22	1036	Loss	0.339	Loss	missense	5	152	CCG (P)	CTG (L)
23	1037	Loss	1.139	Loss					
24	1039	Loss	0.922	Loss	deletion (6)	7	235	AAC (N)	ATG (M)

Two patients, sample numbers 10 and 11, showed hemizygous loss of the *miR-22* gene locus with intact *TP53*. Three patients, sample numbers 1, 5, and 12, showed downregulation of *miR-22* with intact *TP53*.

cancer (Fig. 1A and Supplementary Fig. S1E). Two of them, *miR-22* and *miR-101*, showed strong inhibition of cell proliferation in HCT 116-p53$^{+/+}$ cells by MST assay (Fig. 1B). As shown in Fig. 1C, *miR-22* and *miR-101* showed reduced expression in 70.8% and 50.3% of colon cancer cases, respectively, when compared with their normal counterparts. *MiR-22* also showed significant downregulation in 6 colon cancer cell lines in comparison with FHC cells derived from normal colon epithelium (Fig. 1D), which was not observed for *miR-101* (data not shown). Interestingly, CGH analysis showed deletion of the *miR-22* locus without loss or mutation of *TP53* localized to the 6Mb centromeric region of the *miR-22* gene in 2 colon cancer patients, and 3 other cases showed a significant reduction of *miR-22* expression (Fig. 1E and Table 1). Furthermore, in a copy number assay using another set of colon cancer samples, 5 of 36 cases showed hemizygous deletion of *miR-22* locus with intact copy of *TP53* (Supplementary Fig. S2).

Induction of apoptosis by *miR-22* in p53 wild-type colon cancer cells

Cell proliferation assays using the HCT 116-p53$^{+/+}$, HCT 116-p53$^{-/-}$, and p53 mutant SW480 cell lines showed a significant repression of cell proliferation by *miR-22* in 3 cell lines (Supplementary Fig. S3A). Interestingly, *miR-22* induced apoptosis selectively in HCT 116-p53$^{+/+}$ cells (Fig. 2A and B). In contrast, it caused cell-cycle arrest in HCT 116-p53$^{-/-}$ and SW480 cells (Supplementary Fig. S3B and C). These results indicate that *miR-22* acts as a growth repressor in colon cancer cells, and that its ability to induce apoptosis depends on the *TP53* status. Indeed, the expression profile of HCT 116 cells in the presence of *miR-22* showed significant modulation of

Published OnlineFirst May 12, 2011; DOI:10.1158/0008-5472.CAN-10-2475

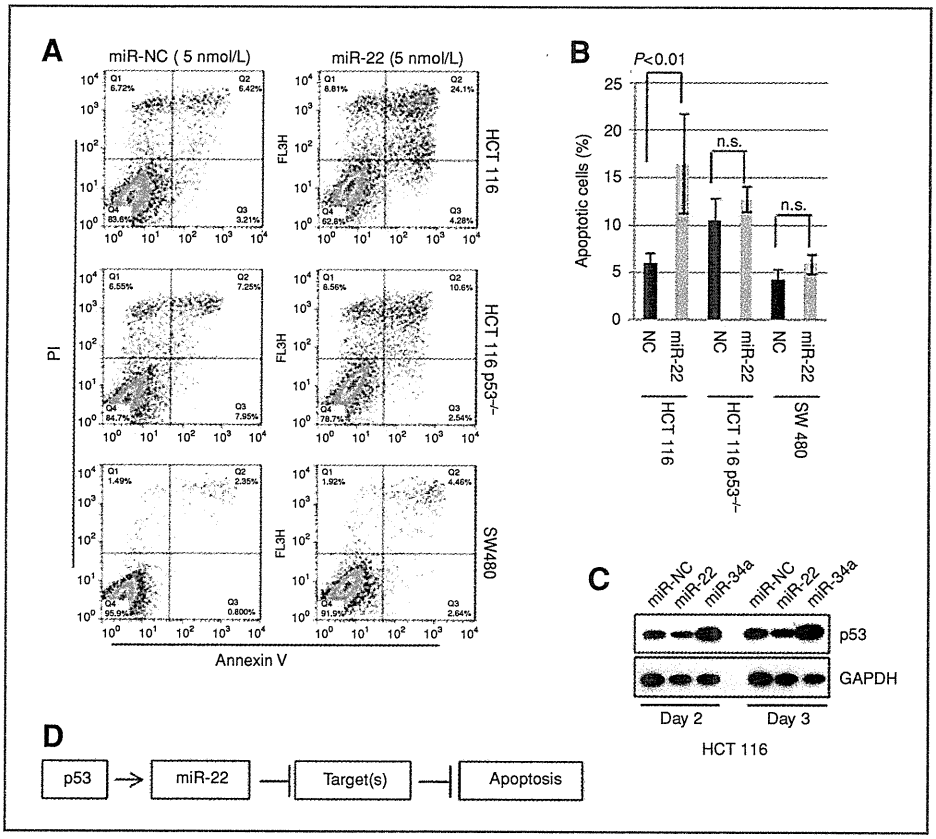

Figure 2. A, fluorescence-activated cell sorting (FACS) analysis. HCT 116, HCT 116-p53$^{-/-}$, and SW480 were transfected with 5 nmol/L of *miR-22* or miR-NC, incubated for 3 days, and subjected to FACS analysis. B, quantification of apoptotic cells. Apoptotic cells were quantified by using 4 independent FACS experiments. Data indicate the mean value with SD. Statistical analysis was carried out by *t* test. C, p53 is not activated by *miR-22*. Cells, transfected with *miR-22* or miR-NC, were incubated for 2 or 3 days, and subjected to immunoblotting. D, hypothesis of *miR-22* function in the p53 network.

cellular p53 network (Supplementary Fig. S3D and Tables S3 and S4). Furthermore, the introduction of *miR-22* into HCT 116 cells did not show upregulation or stabilization of p53, suggesting that *miR-22* may function downstream of the p53-induced apoptotic pathways, and that its role in the induction of apoptosis could be mediated by the repression of p53 target genes (Fig. 2C and D).

Identification of the *miR-22* gene as a direct transcriptional target of p53

As shown in Fig. 3A, *miR-22* is encoded within exon 3 of the *C17orf91* gene, which is located on the minus strand of the 17p13.3 region of the human chromosome, and consensus sequence of p53 binding sites (p53BS) was identified at a 5′ upstream region and within the intron 2 of the *C17orf91* gene (Fig. 3A and Supplementary Fig. S4). The expression of *miR-22* was assessed in HCT 116-p53$^{+/+}$ cells treated with 100 ng/mL of Adriamycin (ADR; doxorubicin, Bedford Laboratories), a genotoxic agent leading to activation of p53, for 24 hours. The result indicated that mature *miR-22* was increased considerably by ADR treatment in HCT 116-p53$^{+/+}$ cells, but not in HCT 116-p53$^{-/-}$ cells (Fig. 3B). The expression of *C17orf91* was induced only in HCT 116-p53$^{+/+}$ cells by ADR (Fig. 3C). Transcriptional activation of *miR-22* was also found in HCT 116 cells after treatment with 5-FU, which was confirmed by qRT-PCR and reporter gene analyses (Supplementary Fig. S5A–C). Furthermore, introduction of a cDNA encoding *C17orf91*, cloned by using a gene-specific primer set (Supplementary Fig. S4), into cells clearly showed an increase of mature *miR-22* in both p53 wild-type and p53$^{-/-}$ HCT 116 cells (Fig. 3D). These results suggest that *miR-22* expression is regulated by p53 at the transcriptional level, not by p53-dependent processing during the maturation of the miRNA (32). Indeed, p53 binding on p53BS located at 5′ upstream and intron 2 of the *miR-22* gene was significantly enhanced after exposure to 5-FU evidenced by p53 ChIP (Supplementary Fig. S5D and E). Furthermore, this was also confirmed by ChIP-sequencing (ChIP-Seq) analysis (Fig. 3E), indicating that *miR-22* is a direct transcriptional target of p53. The concurrent increase in tri-methylation of lysine 4 of histone H3 (33) evidenced transcriptional activation of the *miR-22* gene after exposure to 5-FU (Fig. 3E).

Identification of *p21* as a direct target of *miR-22*

To identify the *miR-22* target mRNAs involved in p53-dependent apoptosis, AGO2-immunoprecipitation (AGO2-IP) on ChIP analysis (31) was applied to screen mRNA species enriched in the AGO2 complex in a *miR-22* dependent manner; an *in silico* database search was further carried out using candidate mRNAs. This strategy was expected to lead to the efficient identification of responsible miRNA

Published OnlineFirst May 12, 2011; DOI:10.1158/0008-5472.CAN-10-2475

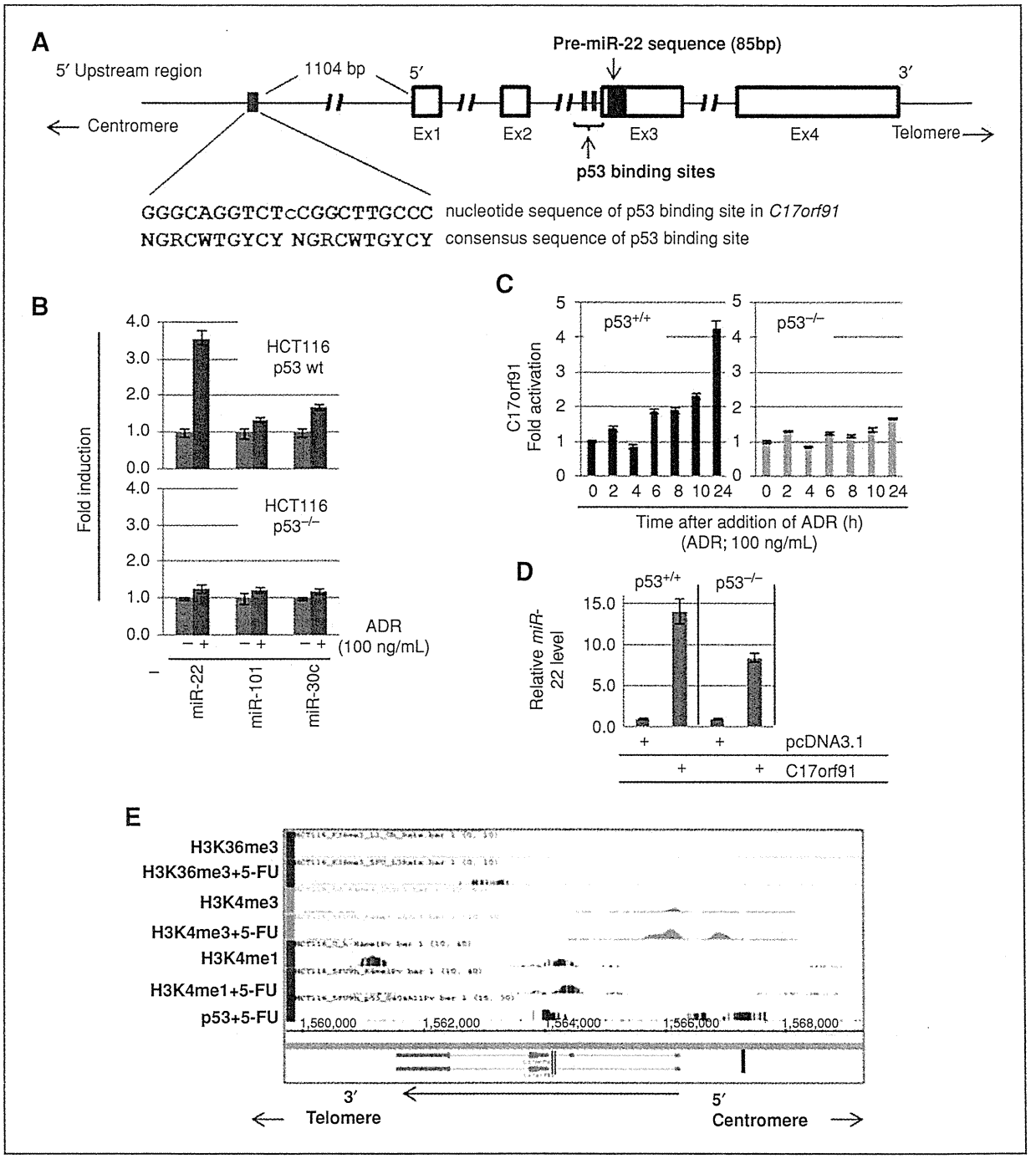

Figure 3. A, genomic structure of *miR-22* and its host gene, *C17orf91*. Genomic structure of C17ORF91 is indicated. Open boxes show exons and the region-encoded pre-*miR-22* is indicated by a closed box. Red boxes are p53 binding site at 5′ upstream region and within intron 2. Consensus sequences of p53 binding sites located 5′ upstream of exon1 of *C17orf91* are shown. B, induction of *miR-22* expression after addition of the genotoxic agent ADR in p53-wild type (wt) and p53$^{-/-}$ HCT 116 cells. Cells were cultured in the presence or absence of ADR (100 ng/mL) for 24 hours. Mature-type miRNAs were measured by qRT-PCR. *miR-101* and *miR-30c*, whose expression was not affected by p53, were used as negative controls. C, upregulation of *C17orf91* by ADR. The cells were treated with ADR (100 ng/mL) for the indicated times, and *C17orf91* was quantified by TaqMan qRT-PCR. D, upregulation of *miR-22* by introduction of *C17orf91* cDNA. Cells were transfected with an expression vector containing *C17orf91* cDNA (Supplementary Fig. S4) for 48 hours. The expression of *miR-22* was analyzed by qRT-PCR. E, ChIP-sequence analysis. Genomic region of C17orf91 indicates opposite direction as shown in (A) because of C17orf91 gene encoded on minus strand in the chromosome 17. HCT 116 cells were treated with a DNA-damaging agent, 5-FU, for 9 hours, and ChIP was carried out by using the indicated antibodies. Red boxes show p53BS located at 5′ upstream region and within intron 2. The direction of *C17orf91* gene is indicated by arrows.

Published OnlineFirst May 12, 2011; DOI:10.1158/0008-5472.CAN-10-2475

targets. HCT 116 cells, stably expressing HA-AGO2, were transfected with *miR-22*, and the AGO2 complex was precipitated with anti-HA antibody, followed by the microarray analysis of the precipitated RNAs (Supplementary Fig. S6A). After calculation of the enrichment score (Supplementary Fig. S6B), 10 mRNAs were selected as *miR-22*–dependent AGO2-bound mRNAs, which included regulators of apoptosis and the cell cycle (Supplementary Fig. S6C and D). A search of the TargetScan database (34) using the top10 mRNAs revealed that only *p21* was a potential target for *miR-22*. Indeed, *p21* had a potential *miR-22* target sequence, whose site was conserved among the other mammalian species (Fig. 4A and Supplementary Fig. S6E). The expression of a luciferase reporter gene fused with the 3′ UTR of *p21* mRNA was suppressed by the introduction of *miR-22* (Fig. 4B). This suppression was significantly reduced by the introduction of mutations into the *miR-22* response sequence (Fig. 4B, Mut1 and Mut2), indicating that *miR-22* represses *p21* directly. Furthermore, ectopic expression of *miR-22* in HCT 116-p53$^{+/+}$ cells reduced p21 protein levels (Fig. 4C). Suppression of *p21* mRNA levels was also observed by introduction of *miR-22* (Fig. 4D). These results show that *miR-22* controls *p21* expression by both inhibition of translation and degradation of mRNA.

As shown in Fig. 4E, *miR-22* inhibited the ADR-induced upregulation of p21. Immunocytochemical analysis showed no nuclear accumulation of p21 in *miR-22* introduced cells, even after a 10-hour ADR treatment (Fig. 4F). To show that this repression occurs at a post-transcriptional, but not at a transcriptional level, the ADR-induced increase in *p21* mRNA was quantitatively assessed in the presence or absence of *miR-22*. As expected, transcriptional activation of *p21* was observed with similar kinetics as the p53 response in both miR-NC and *miR-22* introduced cells after ADR treatment (Fig. 4G). These observations suggest that *miR-22* directly represses *p21* expression via a post-transcriptional mechanism.

Sensitization of p53-dependent apoptosis by *miR-22*

p21 is known to be a key regulator of cell-cycle arrest after the activation of p53, and also an inhibitor of apoptosis (35). Thus, we analyzed the effect of *miR-22* levels on the p53-dependent apoptosis. HCT 116-p53$^{+/+}$ cells were transfected with either *miR-22* or miR-NC, and apoptotic cells were quantified by FACS in the presence or absence of ADR. As shown in Fig. 5A, cells transfected with miR-NC showed a slight increase of the Annexin V and PI double-positive fraction after 12-hour exposure to 100 ng/mL of ADR (Fig. 5A, top right and B). The introduction of low amounts (2 nmol/L) of *miR-22* slightly enhanced the induction of apoptosis compared with those with miR-NC in the absence of ADR (Fig. 5A, bottom left, and B). The addition of ADR caused a marked increase of apoptotic cells in *miR-22*–transfected cells (Fig. 5A, bottom right, and B), indicating that *miR-22* sensitizes cells to p53-dependent apoptosis induced by DNA damage. Next, we analyzed the effect of p21 protein levels on *miR-22*-induced apoptosis. *MiR-22* caused significant repression of p21 upregulation by ADR treatment for 24 hours (Fig. 5C, lanes 2 and 5, and Supplementary Fig. S7A). The introduction of p21 ORF showed the reduction of apoptosis, evidenced by the decrease in PARP-1 cleavage (36), in cells transfected with *miR-22* (Fig. 5C, lanes 5 and 11). This was reproducibly detected (Supplementary Fig. S7B).

These results suggest that endogenous levels of *miR-22* are a cellular determinant for the induction of apoptosis through the repression of p21. On the other hand, p21 knockdown induced the cleavage of PARP-1 (Supplementary Fig. S7C). This was consistent with previous reports that p21 deficiency sensitizes cells to apoptosis (37, 38). However, p21 knockdown was not as prominent as is observed by *miR-22* introduction. This strongly suggests that other factors, being also regulated by *miR-22*, could be involved in the sensitization of p53-dependent apoptosis by *miR-22*. Furthermore, inhibition of *miR-22* by expression of an antisense *miR-22* transcript causes the substantial decrease of S-phase cells, suggesting the cell-cycle arrest at G_1 phase (Supplementary Fig. S7D).

Transcriptional activation of *miR-22* depending on the intensity of stresses

To examine whether the expression of *miR-22* and *p21* levels correlate with the induction of apoptosis in a physiologic setting, the kinetics of *miR-22* and *p21* mRNA expression was examined by treating cells with different doses of ADR. As expected, HCT 116 cells treated with 50 ng/mL of ADR showed cell-cycle arrest, but no apoptosis, with rapid increments of *p21* at both mRNA and protein levels; upregulation of *miR-22* was not observed, even after the ADR-mediated activation of p53 (Fig. 6A, left graph, and 6B, left). Under a high-dose exposure to ADR, in contrast, the expression levels of *p21* mRNA and *miR-22* increased from 8 hours after the addition of 200 ng/mL of ADR (Fig. 6A, right). Interestingly, p21 protein levels were not elevated significantly after 36 hours of incubation with ADR, despite the striking increase in *p21* mRNA level (Fig. 6B, top right). The PARP-1 cleavage was observed at a similar kinetics with *miR-22* expression (Fig. 6B). Similarly, a significant activation of *miR-22* accompanying the repression of p21 protein and increase of PARP-1 cleavage was also observed in HCT 116 cells after exposure to high doses of actinomycin D (Act D), an inhibitor of RNA polymerases that activates p53 (ref. 39; Fig. 6C and D). ChIP analysis indicated the enhancement of p53 binding to p53BS in the *miR-22* gene only after addition of high doses of Act D (Supplementary Fig. S8A and B). Interestingly, treatment with deferoxiamine, an inducer of HIF1α that stabilizes and activates p53 (40), did not upregulate *miR-22* or *p21* mRNA and did not induce apoptosis despite the activation of p53 (Fig. 6C and D). These results indicate that the activation of *miR-22* regulated by p53 is dependent on the strength and type of stresses.

Discussion

In the present study, *miR-22* was identified as a strong candidate for tumor suppressor gene in human colon cancers,

Published OnlineFirst May 12, 2011; DOI:10.1158/0008-5472.CAN-10-2475

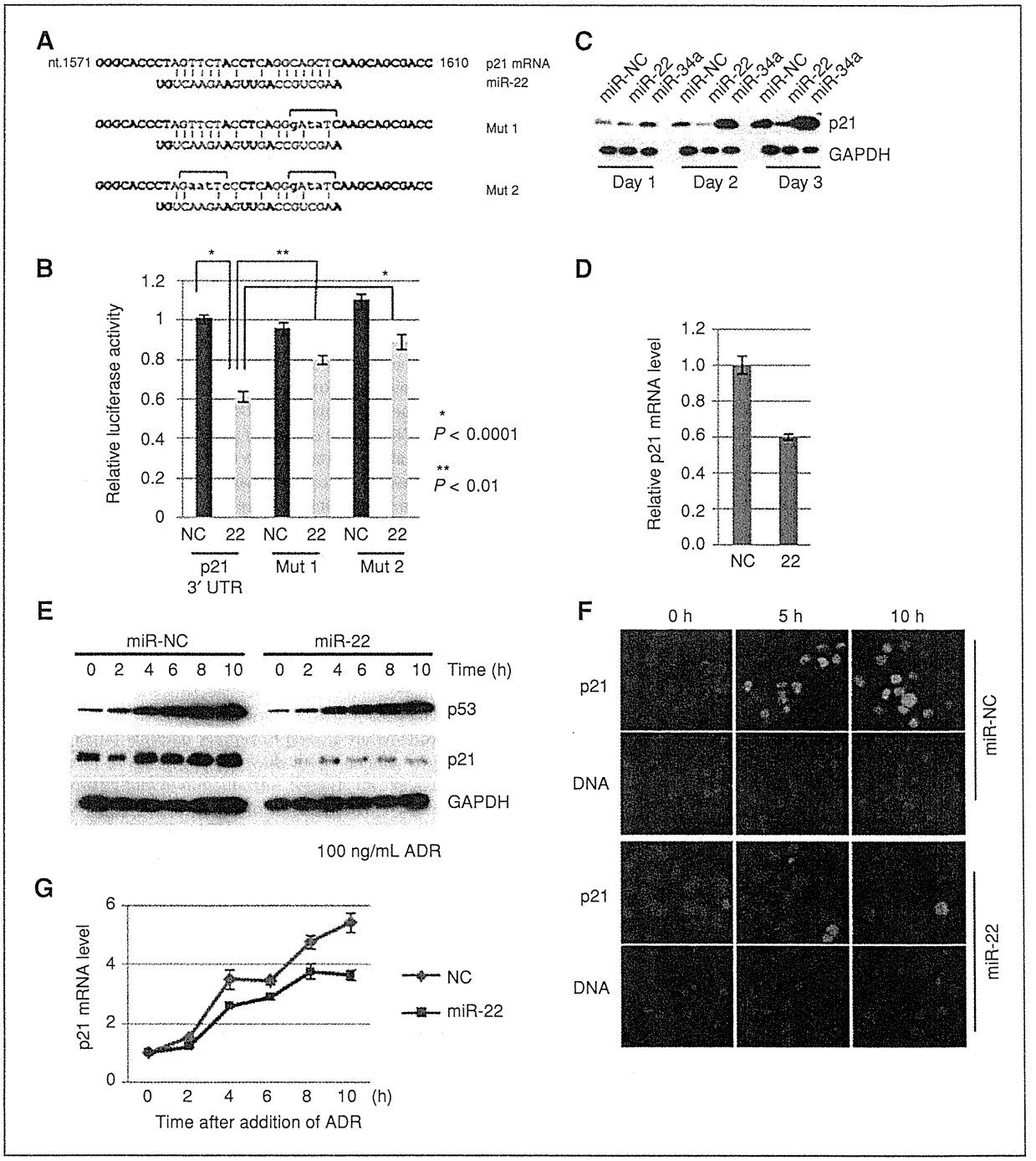

Figure 4. A. sequence alignment of *miR-22* and the 3′ UTR of *p21* mRNA is indicated at the top. Mutant sequences used for the reporter gene assay are listed (Mut 1 and Mut 2). B, reporter gene assay. Error bar indicates SD ($n = 6$). C, expression level of p21 protein in the presence of *miR-22*. *MiR-34a* was used as positive control. D, expression levels of *p21* mRNA in the presence of *miR-22*. Cells were transfected with *miR-22*, and incubated for 3 days. The relative expression levels of *p21* mRNA were quantified by TaqMan assay. E, effect of *miR-22* on the activation of p21 expression after exposure to ADR. HCT 116 cells were transfected with 5 nmol/L of either *miR-22* or miR-NC and incubated for 48 hours, and further incubated in the presence of ADR for the indicated times. F, indirect immunocytochemistry. Cells were transfected as described above, and incubated in the presence of ADR for the indicated times. Cells were subjected to immunostaining. G, activation of *p21* expression in the presence or absence of *miR-22* after exposure to ADR. Cells were prepared as described in (E), and total RNAs were prepared from each time point. Relative expression levels of *p21* mRNA were quantified by TaqMan assay.